Copy 118
RM L50I19

NACA RM L50I19

7213

NACA

RESEARCH MEMORANDUM

THEORETICAL INVESTIGATION OF A PROPORTIONAL-PLUS-FLICKER

AUTOMATIC PILOT

By Ernest C. Seaberg

Langley Aeronautical Laboratory
Langley Air Force Base, Va.

changed to Unclassified

NacaTech Pub Announcement #68
(AUTHORIZED TO CHANGE)

17 Aug 54

By

GRADE OF OFFICER MAKING CHANGE)

11 Apr 61

NATIONAL ADVISORY COMMITTEE
FOR AERONAUTICS
WASHINGTON
October 19, 1950

319.98/13

NATIONAL ADVISORY COMMITTEE FOR AERONAUTICS

RESEARCH MEMORANDUM

THEORETICAL INVESTIGATION OF A PROPORTIONAL-PLUS-FLICKER

AUTOMATIC PILOT

By Ernest C. Seaberg

SUMMARY

The proportional-plus-flicker automatic pilot operates by a non-linear principle whereby a fast-acting flicker servomotor response is combined with a low-speed proportional servomotor response for the purpose of obtaining supersonic stability and control. Essentially, the autopilot maintains a zero reference about which the output is proportional to the input. However, a flicker response overrides this proportional response at a fixed angle of gimbal displacement on either side of the zero gyroscope reference. Therefore, in contrast to other high-speed control systems, the design requirements are simplified because the two components of the proportional-flicker control system are easy to build separately and they can be combined in a relatively simple manner.

By application of the proportional-flicker principle, satisfactory stability can be obtained by the proper adjustment of the variable factors in the autopilot mechanism; namely, the proportional gain, the amplitude of flicker control deflection, the autopilot time-lag factor (the time lag between flicker and proportional operation), and the point in the range that the autopilot switches from a flicker to a proportional system. There is a possibility that these factors can be adjusted so that a more rapid response time (the time to reach steady state) is obtained with the nonlinear proportional-flicker autopilot than with a purely linear proportional autopilot.

For the main part of this analysis, the proportional part of the system is approximated by a zero-phase-lag proportional autopilot with the assumption that the control surface moves instantaneously at the point where the system switches from flicker to proportional. Good correlation is shown between the results obtained by this method and results obtained by using a close approximation of an actual autopilot transfer function for proportional autopilot operation.

The proportional-flicker control system appears to be a practical method for obtaining pitch stabilization of a supersonic pilotless aircraft. Therefore, trials of this system, particularly in supersonic vehicles, appear warranted.

INTRODUCTION

As part of the general research program for investigating various means of automatic stabilization, the Pilotless Aircraft Research Division of the Langley Aeronautical Laboratory has been conducting a theoretical analysis to determine the feasibility of using a proportional-plus-flicker automatic pilot for stabilization and control of a supersonic canard airframe. The principle of operation of this autopilot is believed to be unique because it combines a fast-acting flicker servo response with a low-speed proportional servo response in a relatively simple manner, that is, by overriding the proportional part of the system at a fixed angle of gimbal displacement from the zero gyroscope reference through the use of simple electrical pickoffs attached to the displacement gyroscope outer gimbal.

The reason for attempting to develop an autopilot of this type is to overcome the apparent difficulty in building a high-speed proportional servomotor by the construction of a proportional-flicker servo. Because the fast-acting flicker servo and the low-gain, slow proportional servo by themselves have already been tried and proven, the use of a servomotor combining the two characteristics is suggested, the fast-acting flicker portion to alleviate quickly initial disturbances and to secure a large response quickly to an input signal. The amplitude of flicker control deflection is larger than available from the proportional part, the main function of which is to secure stabilization around the neutral point of the range.

The analysis contained herein pertains to one specific supersonic model configuration for which satisfactory stability was achieved. It is very probable, however, that the optimum adjustments of the variable factors in the autopilot mechanism have not been realized. It is believed that a more complete analysis utilizing an analog computing machine would show the optimum autopilot adjustment more closely. The results of the analysis contained herein show the effects of the following conditions on the stability of the autopilot-model combination based mainly on the flight condition anticipated as a result of previous flight tests of the model:

1. Normal acceleration

2. Aerodynamic out-of-trim moment

3. Static margin, altitude, and Mach number variation

The analysis was continued further to include the response to an initial disturbance and the response to a command signal using approximate physical autopilot transfer functions in the band of proportional autopilot operation.

SYMBOLS

δ canard control-surface deflection, trailing edge down denotes positive deflection, degrees

ϵ error angle between gyroscope frame and instantaneous airframe attitude, degrees

K proportional autopilot gain factor $\left(K = \dfrac{\delta}{\epsilon}\right)$

θ, θ_0 pitch angle measured from horizontal, positive when nose is above the horizontal reference, degrees

$\dot{\theta}$ first derivative of θ with respect to time, degrees per second $(d\theta/dt)$

α angle of attack, positive when nose is up relative to flight path, degrees

$\dot{\alpha}$ first derivative of α with respect to time, degrees per second $(d\alpha/dt)$

γ flight-path angle, degrees $(\gamma = \theta - \alpha)$

g acceleration due to gravity, 32.2 feet per second per second

n normal acceleration in g units

M Mach number

Y stability axis which passes through center of gravity and is perpendicular to vertical plane of symmetry

I_Y moment of inertia about Y-axis, slug feet square

L   lift, pounds

m   mass, slugs; or pitching moment, foot pounds

q   dynamic pressure, pounds per square foot

S   wing area, square feet

c,MAC   mean aerodynamic chord, feet

SM   static margin, feet

V   velocity, feet per second

C_L lift coefficient (L/qS)

C_m pitching-moment coefficient (m/qSc)

C_{L_δ} $\partial C_L/\partial \delta$

C_{L_α} $\partial C_L/\partial \alpha$

C_{m_δ} $\partial C_m/\partial \delta$

C_{m_α} $\partial C_m/\partial \alpha$

$C_{m_{\dot\theta}}$ $\partial C_m/\partial \dot\theta$

$C_{m_{\dot\alpha}}$ $\partial C_m/\partial \dot\alpha$

δ_t value of control-surface deflection which counterbalances
                out-of-trim moment, degrees

m_t out-of-trim moment caused by model misalinement, foot
                pounds

C_{m_t} out-of-trim-moment coefficient (m_t/qSc)

t   time, seconds

τ time-lag factor, seconds

${t_0}^o, {t_5}^o, {t_{10}}^o$ time that the model attitude crosses the point in range
                denoted by subscript, seconds (for example, ${t_0}^o$ signi-
                fies the instant of time that the model attitude θ
                is 0°)

ω   frequency, radians per second

c.p.   model center of pressure

c.g.   model center of gravity

D   differential operator (d/dt)

s   Laplace transform variable corresponding to differential
                   operator

$L^{-1}\left[f(s)\right]$ signifies that inverse Laplace transform of function $f(s)$
                   is to be taken

Subscripts:

.i   input or forcing function corresponding to a command
                   calling for a change in attitude or to a sinusoidal
                   input variation

o   output or response function, for example, system response
                   to a command signal or to a sinusoidal input variation

AIRFRAME AND AUTOPILOT PRINCIPLES AND DESCRIPTION

    A typical qualitative curve of the static servomotor displace-
ment δ plotted against the error signal ε for a proportional-flicker
autopilot system might be as follows:
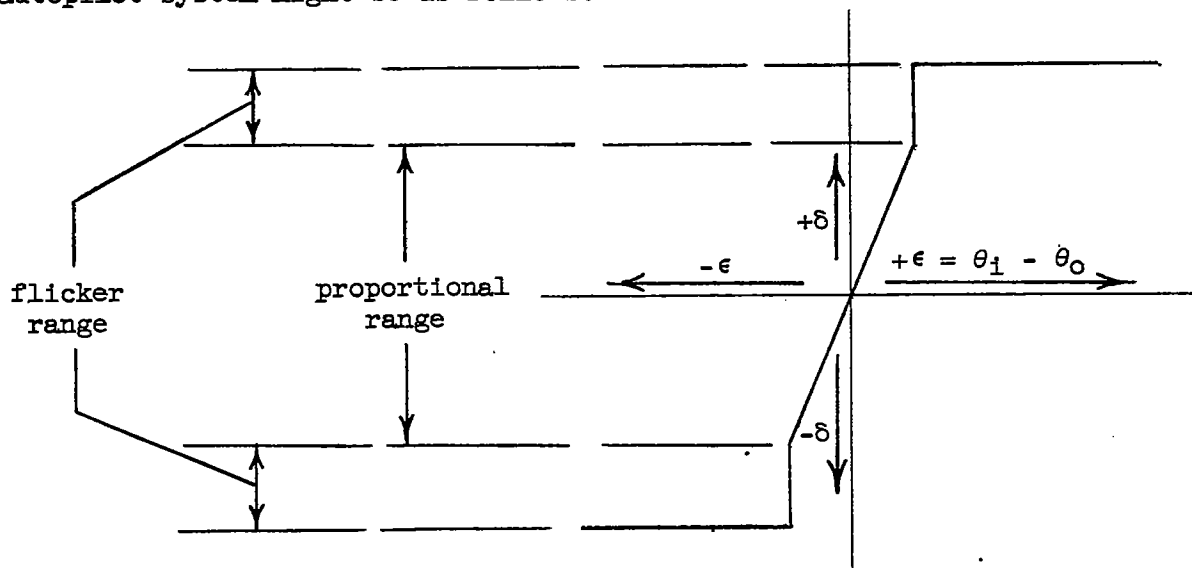
For the theoretical analysis, the estimated pitch derivatives of the canard configuration reported in reference 1 were used. A photograph and plan-view sketch of the model configuration are shown in figure 1.

The autopilot system, as described in the following paragraph, constitutes one method of obtaining a proportional-flicker response, of which many variations are possible. It is also feasible that a completely electric autopilot system could be devised which would function on the proportional-flicker principle.

A schematic diagram of the type of automatic pilot investigated in this analysis is shown in figure 2. This system consists of a displacement gyroscope and a rate gyroscope which transmit error signals to a diaphragm by means of pneumatic Askania pickoffs. (The signal is transmitted by an air jet to either of two holes in the pickoff block, which is connected to the servomotor diaphragm by rubber tubes.) The diaphragm actuates the servomotor slide valve and the servomotor response becomes proportional to the input through the use of a feedback spring. The system thus described constitutes the proportional part of the autopilot, which secures stabilization about the zero gyroscope reference point. The flicker portion of the system is obtained by use of electrical override pickoffs which are mounted on the displacement gyroscope frame and which make contact at a preset angle of displacement with a pickoff attached to the outer gimbal of the displacement gyroscope. (The angle of displacement at which these pickoffs are set determines the switching point and the width of the band of proportional operation about the zero gyroscope reference point.) When either of the flicker pickoffs makes contact, one of the override solenoids is energized which, in turn, actuates the servo slide valve to cause the flicker action of the servomotor piston. The function of the leaf springs in the servo feedback linkage is to alleviate the feedback spring and diaphragm forces during flicker operation. With this arrangement, more rapid flicker action is assured with relatively small solenoids. In operation, a time lag occurs at the autopilot switching point. This causes a delay between proportional and flicker operation when the airframe attitude passes out of the proportional band and causes an overshoot under flicker operation when the attitude crosses the band from the other direction. It is possible to have delay and overshoot periods of different magnitudes.

METHOD OF ANALYSIS

The analysis contained herein consists of calculating the transient responses of the missile-autopilot combination for various initial conditions, approximating those which might be encountered in flight.

The principle on which the proportional-flicker autopilot operates is nonlinear; however, it does lend itself readily to analysis by means of linear approximations and a step-by-step solution, the first step of which is the response to a constant control deflection corresponding to flicker servo action caused by an initial attitude disturbance outside of the proportional band. The airframe motion and corresponding auto-pilot response preceding the initial disturbance were not considered in this analysis. In the initial phase of the calculations, the autopilot operation in the proportional band was approximated with a gyro-actuated control $\left(\frac{\delta}{\epsilon} = K\right)$ of the type used for roll stabilization in reference 1. Calculations based on this assumption are presented in the results as approximations of the actual autopilot-model pitch transient responses to an initial disturbance. Since the actual proportional-plus-flicker autopilot cannot incorporate the use of a gyro-actuated control in the proportional band because the intricacies of the system necessitate the use of a servomotor, further calculations were made using an approximate function $\frac{\delta}{\epsilon} = f(D)$ for the autopilot response in the proportional band. Transient responses incorporating this approximation are also presented in the results.

Three methods of analysis were considered in obtaining the pitch transient responses of the supersonic model-autopilot combination presented in the results. The solution for a constant control-surface deflection applies in the first step of each method. The first method can be generalized as the response to an initial disturbance $\left(\frac{\delta}{\epsilon} = K \text{ in} \right.$ proportional band$\left.\right)$, the second as the response to an initial disturbance $\left(\frac{\delta}{\epsilon} = f(D) \text{ in proportional band}\right)$, and the third as the response to command signal $\left(\frac{\delta}{\epsilon} = f(D) \text{ in proportional band}\right)$.

Response to an Initial Disturbance $\left(\frac{\delta}{\epsilon} = K \text{ in Proportional Band}\right)$

The forms of the equations of motion for constant speed, level flight, are:

$$\left(\frac{I_Y}{57.3qSc} D^2 - C_{m\dot{\theta}} D\right) \theta - \left(C_{m\alpha} + C_{m\dot{\alpha}} D\right) \alpha = C_{m\delta} \delta$$

$$\frac{mV}{57.3qS} D \theta - \left(\frac{mV}{57.3qS} D + C_{L\alpha}\right)\alpha = C_{L\delta} \delta$$

The general solution of these equations is broken down into two steps:
(1) $\delta =$ constant for the flicker portion of the solution, and (2) $\delta = K\epsilon$
for the proportional part of the solution. For both steps the methods
of Laplace (references 2 and 3) were used in obtaining the equation
of θ as a function of time $\boxed{\theta = f(t)}$.

A qualitative example of a typical solution is as follows:
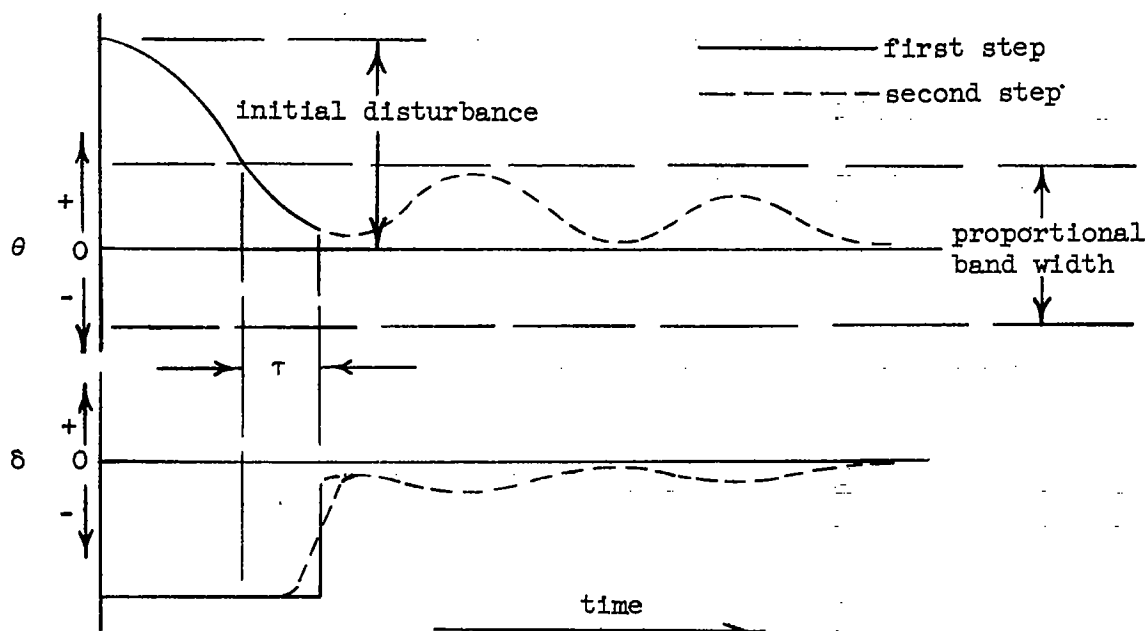
As is shown, the initial disturbance is outside of the proportional
band. Under this condition the control surface δ is against its stop
and the solution for $\delta =$ constant applies until θ crosses the pro-
portional band. At this point a time-lag factor τ is introduced to
allow for the delays in the override solenoid and servomotor. After
this overshoot period the control surface is assumed to move instantane-
ously to a value which corresponds to θ by the relation $\delta = K\epsilon = -K\theta$.
The control surface would actually move as shown by the dotted line.
However, the flicker response is estimated to be at a rate of at least
700° per second; therefore, the step approximation is used because the
solution is simplified, as will be shown, without introducing an appre-
ciable error. At the end of the delay period τ, the proportional
control-surface motion applies and the response is calculated according
to the relation $\delta = K\epsilon$. The initial conditions of this second step are
obtained from the end conditions of the first step. Since the nature of
the solution requires that the initial value of α be known, the tran-
sient $\boxed{\alpha = f(t)}$ for a constant δ was also derived in order to
determine the value of α at the end of the first step.

Response to an Initial Disturbance
$$\left(\frac{\delta}{\epsilon} = f(D) \quad \text{in Proportional Band}\right)$$

This method of solution was derived in order to define more completely the motion of the δ transient at the beginning of the second step. The solution for the first step is identical with that of the first method of analysis and the derivation for the solution of the second step is as follows.

The relations between the airframe and autopilot parameters governing the solution of the second step can be drawn in block diagram form as
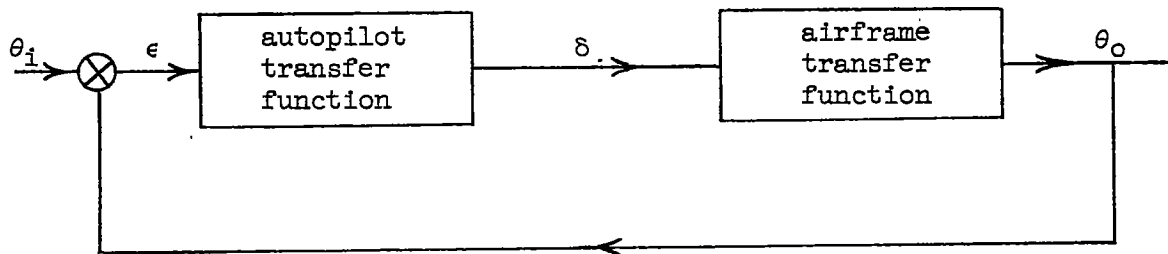
where the transfer functions are functions of the differential operator.

Using the methods of Laplace (references 2 and 3), the equations of motion are transformed to the form

$$f_1(s)\theta_o(s) + f_2(s)\alpha(s) = C_{m\delta}\delta(s) + f_3(s) \tag{1}$$

$$f_4(s)\theta_o(s) + f_5(s)\alpha(s) = C_{L\delta}\delta(s) + f_6(s) \tag{2}$$

where $f_3(s)$ and $f_6(s)$ contain the initial-condition terms.

Expanding equations (1) and (2) and solving for $\theta_o(s)$ yields

$$\theta_o(s) = \frac{f_7(s)\delta(s) + f_8(s)}{f_9(s)} \tag{3}$$

It remains to define $\delta(s)$. By transforming the relation and using $\theta_i = 0$

$$\delta = f(D)\epsilon = -f(D)\theta_o$$

an equation of the form

$$\delta(s) = f_{10}(s)\theta_0(s) + f_{11}(s) \tag{4}$$

is obtained where $f_{11}(s)$ contains the initial-condition terms involving δ and θ_0.

Combining equations (3) and (4) and solving for $\theta_0(s)$ yields

$$\theta_0(s) = \frac{f_{12}(s)}{f_{13}(s)} \tag{5}$$

where $f_{12}(s)$ contains the required initial values of θ, α, and δ and their derivatives. The inverse transform of equation (5) is the transient solution for the second step

$$\theta(t) = L^{-1}\left[\theta_0(s)\right]$$

By combining equations (3) and (4) and solving for $\delta(s)$ an equation defining δ as a function of s can be obtained, the inverse transform of which is the second-step solution for the δ transient response.

Response to a Command Signal

$$\left(\frac{\delta}{\epsilon} = f(D) \quad \text{in Proportional Band}\right)$$

In an automatically stabilized missile, a command signal can be obtained by changing the gyroscope reference point. This command signal may be generated, for example, by the radar unit of a target seeker, by an outside source in a guided missile, or by an altitude control. When the command signal is larger than the proportional band, the flicker portion of the autopilot under consideration will function, yielding a constant control-surface deflection, and the motion will be initiated toward the desired new attitude or new neutral point in the range. An

example of the θ_O variation with time for this third method of analysis might be as follows:
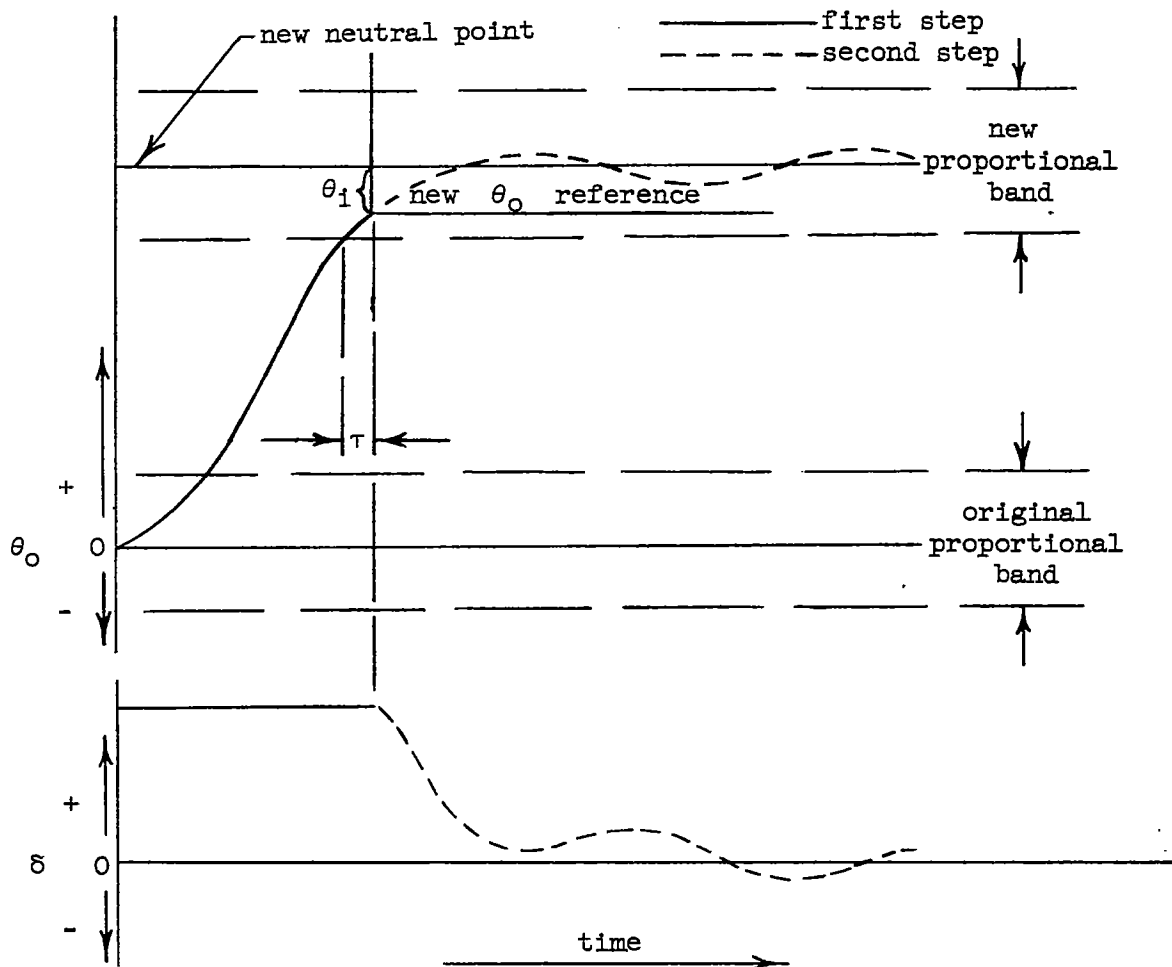
As is shown, the θ_O transient response is assumed to start from level flight and the new neutral point is outside of the original proportional band. Initially the equations of motion are treated in the same manner as in the first step of the first and second method except that the initial value of θ_O is zero. The transient response (θ_O) to a constant δ applies until θ_O crosses the new proportional band. At this point the time-lag factor (τ) is again introduced to complete the first step.

The method of the derivation for the solution of the second step found herein is carried through in general form in references 2, 4, and 5. As mentioned previously, the autopilot frequency response is

approximated by a transfer frunction of the form $\frac{\delta}{\epsilon} = f(D)$ where the error angle (ϵ) is the angle between the gyroscope reference and the instantaneous airframe attitude. The second step, shown as the dotted portion of the θ_O transient response, is the response to a step θ_i where θ_i is the angle between the new neutral point and the value of θ_O at the end of the first step, a new zero reference being taken for θ_O at this point. The equations of motion are handled in the same manner as for the second step of the second method of analysis except that the relation governing the definition of $\delta(s)$ is

$$\delta = f(D)\epsilon = f(D)(\theta_i - \theta_O)$$

therefore, equation (4) becomes

$$\delta(s) = f_{10}(s)\left[\theta_i(s) - \theta_O(s)\right] + f_{11}(s)$$

and the solution for $\theta_O(s)$ takes the form

$$\theta_O(s) = \frac{f_{14}(s)\theta_i(s) + f_{12}(s)}{f_{13}(s)} \qquad (6)$$

The inverse transform of equation (6) gives the solution of the second step of the transient response to a command signal.

The three aforementioned methods of analysis describe the general theories which were derived to obtain the solutions for the transient responses presented in this analysis. Any deviation from these general theories will be described in further detail in the results.

RESULTS AND DISCUSSION

Response to an Initial Disturbance
$\left(\frac{\delta}{\epsilon} = K \text{ for Second Step}\right)$

Determination of the time-lag factor τ.- The time-lag factor for the autopilot previously described is defined as the time that it takes for flicker servo action after the flicker-actuating solenoid has been energized or deenergized. In order to obtain an approximate value of this factor for use in the calculations, a servomotor was constructed which operated on the proportional-flicker principle and which would be suitable for actuating the canard control surfaces of a model of the type which was flight-tested in reference 1. The results of an

experimental test of this servomotor are presented in figure 3. As is shown, an average τ of 0.03 second was obtained. It is not believed that more rapid flicker actuation can be obtained with this type of system due to the limitations on the size of solenoids; however, it would not be difficult to increase the time-lag factor if necessary for stability.

Determination of the proportional gain and amplitude of flicker control deflection.- For these calculations the coefficients and model longitudinal pitch derivatives were estimated on the basis of sea-level flight at a Mach number of 1.8 with the static margin equal to 0.86c or approximately 14 inches. The geometric characteristics and estimated derivatives used are given in table I.

A detailed description of the steps required for a solution such as shown in figure 4 is as follows: The first step is the response to a constant δ. The second step which starts at some time after the model attitude passes the proportional boundary is governed by the approximate relation $\delta = -K\theta$ for the major part of this analysis. This simplifies the calculations and still gives a good approximation of the actual θ response. The values of the initial-condition terms necessary for the second-step solution of the equations of motion are obtained from their values at the end of the first step. If the θ response stays inside the proportional band and the motion dies out, the solution is complete in two steps. However, if the model attitude again reaches the proportional band, the flicker-actuating solenoid will be energized, making more steps necessary. For the third step the δ response is assumed to hold a constant value which is determined from the relation $\delta = -K\theta$ where θ is the proportional band limit. The initial-condition terms are again found from their values at the end of the previous step. The time-lag factor determines the duration of the third step. When this period of time has elapsed the fourth step is initiated for which the constant flicker δ applies as in the first step. This step-by-step solution is continued until the response of the model-autopilot combination is determined.

The first calculated transient responses, presented in figure 4, were based on a flicker δ of $\pm10^\circ$, a proportional band of $\pm5^\circ$ which is designated in this and subsequent figures by the long-dashed lines, and a time-lag factor of 0.03 second. The initial pitch disturbance for the curves presented in this figure was 9° and the value of K was -1 for figures 4(a) and 4(b), while in figures 4(c) and 4(d) K = -0.3 where K is equal to the control-surface gain ratio δ/ϵ. Figure 4(a) shows the response when the first step ends at 0.03 second after the model attitude θ passes the proportional boundary ($+5^\circ$), designated by $t_5{}^\circ + 0.03$ second on the figure. Figure 4(b) shows the response when the first step ends at 0.03 second after the model attitude passes through the neutral point (0°) or $t_0{}^\circ + 0.03$ second. This would

CONFIDENTIAL

necessitate a more intricate flicker-actuating pickoff and relay system than that shown in figure 2; however, its development would not propose a major problem. As can be seen in both figures 4(a) and 4(b), the response is unstable as is indicated by the divergent transient oscillations. Curves for the same conditions are shown in figures 4(c) and 4(d) except that $K = -0.3$ in the proportional band. As can be seen, decreasing the gain in the proportional band does not increase the stability but actually has the effect of making the model-autopilot combination more unstable.

Since it is apparent that a flicker control-surface gain of $\pm10^\circ$ is too high for stability at $M = 1.8$, calculations for a lower flicker gain, namely $\pm5^\circ$, were made. Curves based on a flicker δ of $\pm5^\circ$ and on the same derivatives used for figure 4 are presented in figure 5. The curves of figure 5(a) show that, for an initial disturbance of $\theta = 9^\circ$, proportional band of $\pm5^\circ$, and for $K = -0.3$, the transient response is undesirable when the first step ends at $t_5^\circ + 0.03$ second, but when the switching point is extended to $t_0^\circ + 0.03$ second the transient response is stable. The secondary oscillation which appears during the second step is induced by the instantaneous movement of the control surface δ. Figure 5(b) shows that, for a larger K (namely, for $K = -1$), the proportional band can be smaller $(\pm3^\circ)$ and the response will still be stable and damp out in two steps. For a smaller initial disturbance, however, the stability is more critical, as is shown by the curve which has an initial disturbance of $\pm5.5^\circ$. For this reason the curve shown in figure 5(c) was calculated for an initial disturbance which is just outside of the proportional band, namely, an initial disturbance of $\pm3.5^\circ$ for a proportional band of $\pm3^\circ$. As is shown, the calculated transient response is divergent; however, by increasing the time-lag factor τ to 0.1 second as in figure 5(d) the transient is made to stay inside the proportional band in the second step. Actually, the autopilot in this instance could have two values of τ, 0.03 second when the attitude passes out of the proportional band, and 0.1 second when the attitude crosses 0°.

Since it appears that a stable transient response can be obtained by the proper adjustment of the variable factors in the autopilot mechanism, it was decided to increase the flicker control-surface gain to $\pm7^\circ$ in order to obtain the advantage of a more rapid response time than that obtained with a gain of $\pm5^\circ$. For this reason the analysis of the calculated transient responses which follows will be based on a flicker δ of $\pm7^\circ$ and a proportional band of $\pm4^\circ$. The first responses for these conditions, shown in figure 6, were calculated using $K = -1$ in the second step with the first step ending at some time after the model attitude has passed through the zero gyroscope reference. In this instance, the autopilot will function as a proportional system as long as the initial disturbance is within the $\pm4^\circ$ boundary. In the event that

the model attitude passes either side of these limits, the flicker
control surface of $\pm 7^\circ$ will apply, whichever is corrective. The flicker-
actuating solenoid will be deenergized and proportional control will
again apply some time after the model attitude passes through the zero
gyroscope reference. Proportional-flicker transient responses to a 9°
initial θ disturbance were calculated with the first step ending at
$t_0^\circ + 0.03$ second and at $t_0^\circ + 0.1$ second, as shown in figure 6. In
this particular instance, the larger time lag yields a transient
response which is closer to the zero θ reference. The upper curve on
figure 6 shows the response of a zero phase lag proportional autopilot
$\left(\dfrac{\delta}{\epsilon} = K \text{ for the entire curve} \right)$. This curve serves to illustrate the dif-
ference between the response obtained from a linear autopilot and the
responses obtained with the proportional-flicker autopilot. For the
particular value of autopilot gain used in calculating the response
obtained with the zero phase lag proportional autopilot, the
proportional-flicker responses, although more oscillatory, are more
rapid than the pure proportional autopilot response. The value of K
used for the zero-phase-lag proportional autopilot response was -0.6.
The choice of this autopilot constant was based on the method suggested
in reference 5. This method is illustrated in figure 7 where the
Nyquist diagram with a K of -0.69 is shown to be tangent to, and not
greater than, the locus of points required to make the peak amplitude
ratio of the model-autopilot combination 1.3.

Acceleration effects.- Normal acceleration and θ, α, and γ
transient responses for the model-proportional-flicker-autopilot com-
bination are presented in figure 8. The θ transient is the curve with
the first step ending at $t_0^\circ + 0.1$ second, as shown previously in fig-
ure 6. As is shown, the trim α is about -2.5° and the steady-state
normal acceleration is approximately -11g for the first step, with a
peak acceleration overshoot of about -18.8g.

An indication of the model aerodynamic loads to be expected under
flicker-autopilot operation can be obtained from the steady-state varia-
tion of n/δ with static margin for a constant δ input, as shown in
figure 9 for sea-level flight. This curve is based on the variation of
the model longitudinal derivatives with center-of-gravity location
at $M = 1.8$. Figure 9 shows only the steady-state acceleration; however,
the peak acceleration is the design factor, therefore acceleration
curves such as the one shown in figure 8 are necessary to estimate the
amount of acceleration overshoot. The method employed in deriving the
relation on which the plot of n/δ against static margin is based is
given in appendix A.

The effect of out-of-trim moment.- The value of the out-of-trim
moment is assumed to be that which will give a certain value of δ
out of trim (δ_t) or

$$m_t = C_{m_\delta}\delta_t qSc$$

The out-of-trim moment coefficient $\left(C_{m_t}\right)$ is therefore defined as

$$C_{m_t} = C_{m_\delta}\delta_t$$

This coefficient has the effect of adding another term to the moment equation as follows:

$$\left(\frac{I_Y}{57.3qSc}D^2 - C_{m_{\dot\theta}}D\right)\theta - \left(C_{m_\alpha} + C_{m_{\dot\alpha}}D\right)\alpha = C_{m_\delta}\delta + C_{m_t}$$

The solution of this equation, combined with the lift equation, for each step of the proportional-flicker transient responses shows the effect of introducing an assumed value of an out-of-trim moment.

Transient responses, including the effect of an out-of-trim moment, are shown in figures 10 and 11. These figures are based on sea-level flight at $M = 1.8$ and with $SM = 0.86c$, and the initial θ disturbance was $4.5°$ with K equal to -1 for the second step. It is shown in figure 10(a) that, without the out-of-trim effect, the model-autopilot transient response is made to damp out in the second step when the time-lag factor is increased to 0.1 second, that is, when the first step ends at 0.1 second after the model attitude has passed through the neutral point ($0°$). Therefore, the remaining curves shown in figures 10 and 11 are based on the value $t_0 + 0.1$ second for the length of the first step. Figure 10(b) shows the responses when out-of-trim moment coefficients of -0.012 and +0.012 are used. These values of C_{m_t} cause the θ transients to trim about $-0.57°$ and $+0.57°$, respectively. However, the stability is not affected to any great extent since the response is damped to within approximately $1°$ of the trim value in 0.6 second in each case. More severe values of C_{m_t}, namely, +0.058 and -0.058, were used in figure 11. These give trim θ values of $+2.87°$ and $-2.87°$, respectively, which are only $1.13°$ from the proportional boundary limits ($\pm 4°$). However, although the responses take longer to damp to the new trim values, they are still stable and stay inside the proportional band in the second step. For comparison, calculated transient responses including an out-of-trim moment and based on a zero-phase-lag proportional autopilot with $K = -0.6$ are also shown in figure 11. For these curves a C_{m_t} of ± 0.035 was used because, for comparison, it is desirable that the trim θ ($\pm 2.87°$) be the same as for the proportional-flicker responses. In figure 11(a) it is shown that, since the proportional-flicker response must first pass through $0°$ and then oscillate back to the trim value, the response is not much faster than the pure proportional autopilot response. However, in figure 11(b) where the out-of-trim moment is negative, the proportional-flicker autopilot has the more rapid response time.

The response to an initial disturbance including initial values of $\dot\theta$ and α.- An initial pitching velocity $(\dot\theta)$ of 50 degrees per second and an angle of attack (α) of 0.5° were used for the results presented in figure 12. These are representative of the values which might be encountered along the flight range of the type of model being used in this analysis. In figure 12(a) the initial $\dot\theta$ was 50 degrees per second with zero initial angle of attack, while in figure 12(b) initial values of both $\dot\theta$ and α were used and the variation of normal acceleration and α with time are also shown. The stability of longitudinal transient responses is not affected greatly by including the effect of these initial conditions.

The effect of Mach number change.- In order to determine the stability characteristics of the model-proportional-flicker-autopilot combination for a different Mach number, the derivatives for $M = 1.4$ were estimated as given in table I for the same center-of-gravity location resulting in a static margin of $0.9c$. Results based on these derivatives are presented in figure 13 as θ and α transient responses to 9° and 4.5° initial pitch disturbances. The θ transients are comparable, except for Mach number, to the curves with the first step ending at $t_0^\circ + 0.1$ second shown previously in figures 6 and 10(a) and, although the response time is a little slower, the results of figure 13 show stability.

The effect of static-margin reduction.- The constants and aerodynamic derivatives used for the curve presented in figure 14 were based on sea-level flight at $M = 1.8$ and $SM = 0.3c$ and are given in table I. This amounts to a decrease in static margin from approximately 14 inches to 5 inches. As is shown, an undesirable result is obtained because the θ transient response does not die out in the second step. Instead, the response diverges until what appears to be a pure flicker response is obtained. Therefore, in a system of this type, the problem of obtaining a more rapid response time is not solved by simply decreasing the static margin.

The effect of altitude variation.- Except for altitude, the proportional-flicker response with the first step ending at $t_0^\circ + 0.1$ second, shown in figure 6, is comparable to the curves presented in figure 15 where the pitch transient responses to a 9° initial θ disturbance are based on flight at 10,000 and 25,000 feet. As is shown, flight at altitude produces a slower response time but does not appreciably affect the stability of the model-autopilot combination because, in both cases presented in figure 15, it is indicated that the transient response will die out in the second step.

Response to an Initial Disturbance

$$\left(\frac{\delta}{\epsilon} = f(D) \quad \text{in Proportional Band}\right)$$

Determination of the approximate autopilot functions.- The method
employed to determine mathematical transfer functions which approximate
the autopilot amplitude and phase response was as follows: First, the
experimental autopilot amplitude and phase responses were obtained from
oscillating-table tests of actual autopilots. Two autopilots were used
in this analysis. The first consisted of the servomotor used previously
to obtain the experimental results presented in figure 3, and the
oscillating-table error angle was measured by a German V-1 displacement
and rate gyroscope which generates the input to the servomotor by the
use of pneumatic Askania pickoffs. The autopilot amplitude and phase
test points, thus obtained, were then plotted on semilog paper using a
decibel scale for the amplitude response. Transparent templates based
on plots of known quadratic and linear functions on this same semilog
paper were then used until the combination of templates which most
closely matched the autopilot test points was determined. The method
used to make the log magnitude and phase templates and explanations of
their applications are found in chapter 8 of reference 2.

The approximate autopilot transfer function obtained by the afore-
mentioned method is

$$\frac{\delta}{\epsilon} = \frac{225(D + 27.2)}{\left(D^2 + 141D + 7744\right)}$$

This function will then govern the proportional part of the proportional-
flicker transient responses. A comparison of this approximate function
with the autopilot test points based on the amplitude and phase response
of the proportional-flicker servomotor obtained from oscillating-table
tests of a V-1 displacement and rate gyroscope is presented in figure 16.
The agreement between the approximate function and the experimental
results can be seen in figure 16(a), where the approximate autopilot
transfer function and the autopilot test points for oscillating-table
amplitudes of $\pm 1.13^\circ$, $\pm 3.03^\circ$, and $\pm 4.85^\circ$ are plotted on linear coordi-
nates. The experimental results vary with oscillation amplitude due to
the nonlinearities of the autopilot mechanism. However, the agreement
between the mathematical function and the experimental results is sat-
isfactory except for the low-amplitude oscillations ($\pm 1.13^\circ$), where the
amplitude response peaks more sharply.

A further comparison between the approximate autopilot transfer
function and the actual autopilot test points is made in figure 16(b)
in the form of Nyquist diagrams, where the mathematical function and
the test points are combined with the model transfer function to obtain

the loci of the polar plots. The model transfer function is based on
sea-level flight at M = 1.8 and with SM = 0.86c. Satisfactory agree-
ment is again shown between the approximate autopilot transfer function
and the experimental results except for the Nyquist plot based on the
±1.13° test points.

The second approximate autopilot mathematical transfer function was
based on the amplitude and phase response of a servomotor using a dis-
placement gyroscope only to generate the input signal. This approximate
function is

$$\frac{\delta}{\epsilon} = \frac{2880}{D^2 + 156D + 3600}$$

and it is compared with the autopilot consisting of a displacement
gyroscope plus servomotor in figure 17. Autopilot test points are
plotted for oscillating-table amplitudes of ±4.2° and ±2.15°, and satis-
factory agreement with the plot of the approximate mathematical function
is shown.

Autopilot containing displacement-plus-rate gyroscopes.- As shown
previously in the method of analysis section, the function $\delta(s)$ and
the initial values of the δ derivatives are included in the derivation
of the $\theta_0(s)$ function in the second method of analysis. Although the
manual solution for the θ and δ transient responses are much more
involved when using this type of derivation, it is of value because it
yields a more complete definition of the control-surface motion.

Figure 18 shows the pitch transient responses to different initial
θ disturbances based on the longitudinal derivatives given in table I
for sea-level flight at M = 1.8 and with SM = 0.86c. The flicker
gain is ±7° and the proportional band is ±4°. In figure 18(a), the
initial θ disturbance is 10° and the first step ends at 0.03 second
after the model attitude has passed through the neutral point (0°). In
this figure the calculated δ response is also shown. In figure 18(b)
the initial θ disturbance is 4.5° with curves shown for the first step
ending at $t_0^{\circ} + 0.03$ second and $t_0^{\circ} + 0.1$ second. The δ response is
plotted for the case where the first step ends at $t_0^{\circ} + 0.03$ second.
As is shown, the smaller time-lag factor (0.03 second) is more critical,
with the second oscillation of the θ transient actually crossing the
proportional band. This would ordinarily necessitate handling the
solution with more than two steps. However, it would be necessary to
know the initial value of α for the third step and, since the charac-
teristic equation for the α transient when $\frac{\delta}{\epsilon} = f(D)$ is tenth order,
a manual solution was not attempted. It is more desirable to obtain a
less oscillatory transient response which damps out in two steps by

increasing the time-lag factor, as is shown for the curve where $\tau = 0.1$ second. Figure 18(c) shows the θ response to a 15° initial disturbance, where for a τ of 0.03 second the motion is damped in two steps.

The agreement between the results shown for the second method of analysis using the autopilot containing displacement-plus-rate gyroscopes and the results shown for the first method of analysis is good. The secondary oscillation which appeared in the second step of the first method of analysis, for example, is also present when using this second method of analysis, resulting in transient responses, the general shapes of which are comparable. On this basis the validity of using the much simpler relation $\frac{\delta}{\epsilon} = K$ for the major part of this analysis seems to be justified.

Autopilot containing displacement gyroscope only.- The second step of the pitch transient responses to 10° and 4.5° initial θ disturbances presented in figure 19 is based on the transfer function

$$\frac{\delta}{\epsilon} = \frac{2880}{D^2 + 156D + 3600}$$

These results show that stability can be obtained with a proportional-flicker autopilot made up of a servomotor and displacement gyroscope only. However, a comparison of figures 18 and 19 shows that the auto-pilot without rate yields a more oscillatory response in the proportional band.

Response to a Command Signal

$$\left(\frac{\delta}{\epsilon} = f(D) \quad \text{in Proportional Band}\right)$$

The response to a command signal.- Pitch transient responses to 4.5° and 10° command signals are shown in figure 20. These responses are based on sea-level flight at $M = 1.8$ and with a static margin of 0.86c. The initial disturbance in each case is larger than the proportional band; therefore, the flicker control setting of +7° applies for the first step of the solution, which ends at 0.1 second after the transient crosses the desired new attitude. In the second step the approximate transfer function

$$\frac{\delta}{\epsilon} = \frac{225(D + 27.2)}{\left(D^2 + 141D + 7744\right)}$$

applies. In figure 20(a) the desired change in attitude is 4.5° or, as explained in the method of analysis section, the transient response shown is the response to a 4.5° command signal. In figure 20(b), the command signal calls for a 10° change in attitude. These results show that stable responses to command signals can be obtained with the proportional-flicker autopilot and the responses appear to be similar, except for direction, to the results for 4.5° and 10° initial disturbances shown in figure 18. A comparison between the proportional-flicker and the zero phase lag proportional response is made for both curves shown in figure 20 and in each case the proportional-flicker autopilot has the more rapid response time.

CONCLUSIONS

The proportional-flicker automatic pilot operates on a nonlinear principle, whereby a high-speed flicker servomotor response is combined with a low-speed proportional servomotor response for the purpose of obtaining stability and control in supersonic flight. Physcially, the autopilot motion operates about a zero reference within two bands. In the inner band, the autopilot output is proportional to the input and a flicker response overrides the proportional response at a fixed angle of gimbal displacement on either side of the zero gyroscope reference. The conclusions arrived at as a result of the analysis conducted herein, based on a specific supersonic model configuration, are as follows:

1. Satisfactory stability can be obtained by the proper adjustment of the variable factors in the autopilot mechanism, namely, the proportional servo gain, the amplitude of flicker control deflection, the autopilot time-lag factor, and the point in the range that the autopilot switches from a flicker to a proportional system.

2. A reasonable aerodynamic out-of-trim moment of the model will not affect the stabilization qualities of the proportional-flicker autopilot to any great extent. Decreasing the static margin appears to have more of an effect on the stability of the proportional-flicker autopilot-model combination. For the same autopilot characteristics, a decrease in static margin from 0.86 to 0.3 mean aerodynamic chord yields a transient response which does not die out but which diverges until what appears to be a pure flicker response is obtained.

3. Good agreement is shown between the response to an initial disturbance using a mathematical transfer function to approximate the autopilot and the method of assuming that the autopilot has a pure proportional response in the proportional band with instantaneous movement of the control surface at the switching point.

4. The proportional-flicker control system can be fabricated and appears to be a practical method for obtaining pitch stabilization of a supersonic pilotless aircraft. Therefore, trials of this system, particularly in supersonic vehicles, appear warranted.

Langley Aeronautical Laboratory
      National Advisory Committee for Aeronautics
            Langley Air Force Base, Va.

APPENDIX A

DETERMINATION OF THE RELATION WHICH EXPRESSES n/δ

AS A FUNCTION OF STATIC MARGIN

The relation

$$C_{m\delta} = C_{L\delta_c} \frac{(x - SM)}{c} + \frac{d\epsilon}{d\delta} C_{L\alpha_W} \frac{(y + SM)}{c} \tag{1}$$

expresses $C_{m\delta}$ as a function of static margin.

From the lift equation, the steady-state value of the normal acceleration in g can be derived for a constant control-surface deflection as

$$n = \frac{1}{32.2m} \left[-C_{L\alpha}qS \frac{C_{m\delta}}{C_{m\alpha}} + C_{L\delta}qS \right] \delta$$

where the steady state α/δ has been assumed to be equal to $-\dfrac{C_{m\delta}}{C_{m\alpha}}$. By incorporating the relation

$$\frac{C_{m\alpha}}{C_{L\alpha}} = \frac{SM}{c}$$

the following relation is obtained, where the variation of the steady-state n/δ is expressed as a function of SM and $C_{m\delta}$

$$\frac{n}{\delta} = \frac{qS}{32.2m} \left[-\frac{C_{m\delta}}{\left(\frac{SM}{c}\right)} + C_{L\delta} \right] \tag{2}$$

For a particular value of SM, $C_{m\delta}$ can be evaluated from equation (1). Then, by using these two values in equation (2), n/δ is determined.

REFERENCES

1. Gardiner, Robert A., and Zarovsky, Jacob: Rocket-Powered Flight
   Test of a Roll-Stabilized Supersonic Missile Configuration.
   NACA RM L9K01a, 1950.

2. Brown, Gordon S., and Campbell, Donald P.: Principles of Servo-
   mechanisms. John Wiley & Sons, Inc., 1948, chs. 3, 8.

3. Churchill, Ruel V.: Modern Operational Mathematics in Engineering.
   McGraw-Hill Book Co., Inc., 1944.

4. James, Hubert M., Nichols, Nathaniel B., and Phillips, Ralph S.:
   Theory of Servomechanisms. McGraw-Hill Book Co., Inc., 1947, ch 2.

5. Hall, Albert C.: The Analysis and Synthesis of Linear Servomechanisms.
   The Technology Press, M.I.T., 1943, chs. 3, 4.

TABLE I

ESTIMATED LONGITUDINAL DERIVATIVES

$\left[\text{All derivatives in degree measure; } I_Y = 37.66 \text{ slug-ft}^2; \right.$
$\left. m = 4.922 \text{ slugs; } c = 1.395 \text{ ft; } S = 2.52 \text{ ft}^2.\right]$

Static margin	Mach number	$C_{m_{\dot\theta}}$	C_{m_α}	C_{m_δ}	$C_{m_{\dot\alpha}}$	C_{L_δ}	C_{L_α}
0.86c	1.8	-0.000138	-0.052	0.204	-0.0000116	-0.000051	0.0607
0.9c	1.4	-.000187	-.0621	.023	-.0000205	-.00105	.0692
0.3c	1.8	-.0000784	-.0181	.0182	-.0000051	-.000051	.0607

VARIATION OF FLIGHT CONDITIONS

Altitude (ft)	Mach number	q (lb/ft^2)	V (ft/sec)
sea level	1.8	4270	1963
sea level	1.4	2902	1562
10,000	1.8	3294	1937
25,000	1.8	1790	1835

L-63726.1
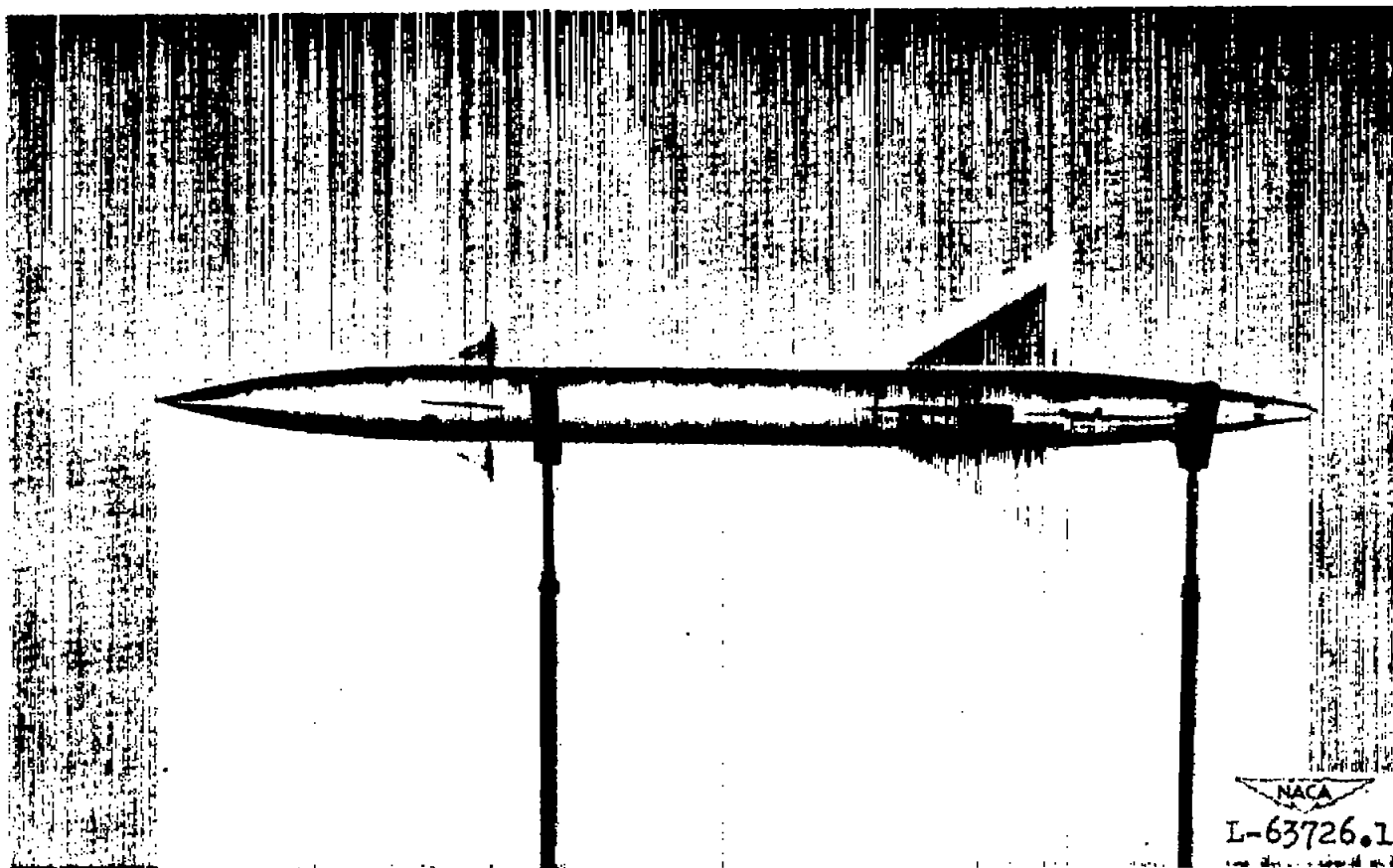
(a) Photograph of model configuration.

Figure 1.- Supersonic missile research model configuration.

Station in inches   0   39   86.2   103   130

M.A.C.

Canard fins

60°

Wing-tip ailerons

Booster
attachment

NACA
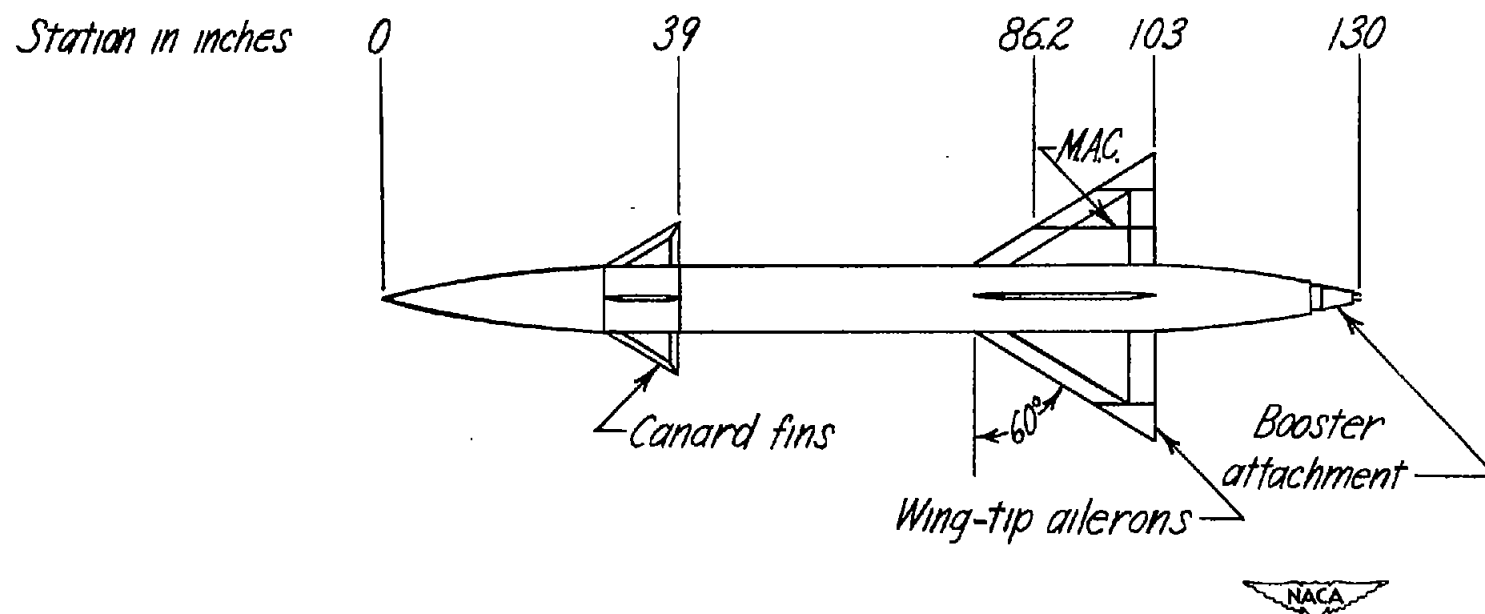
c.p. location
 (station)
  80.42 at M=1.8
  81.03 at M=1.4

(b) Plan-view sketch of model configuration.

Figure 1.- Concluded.

— — — — — — Electrical connection
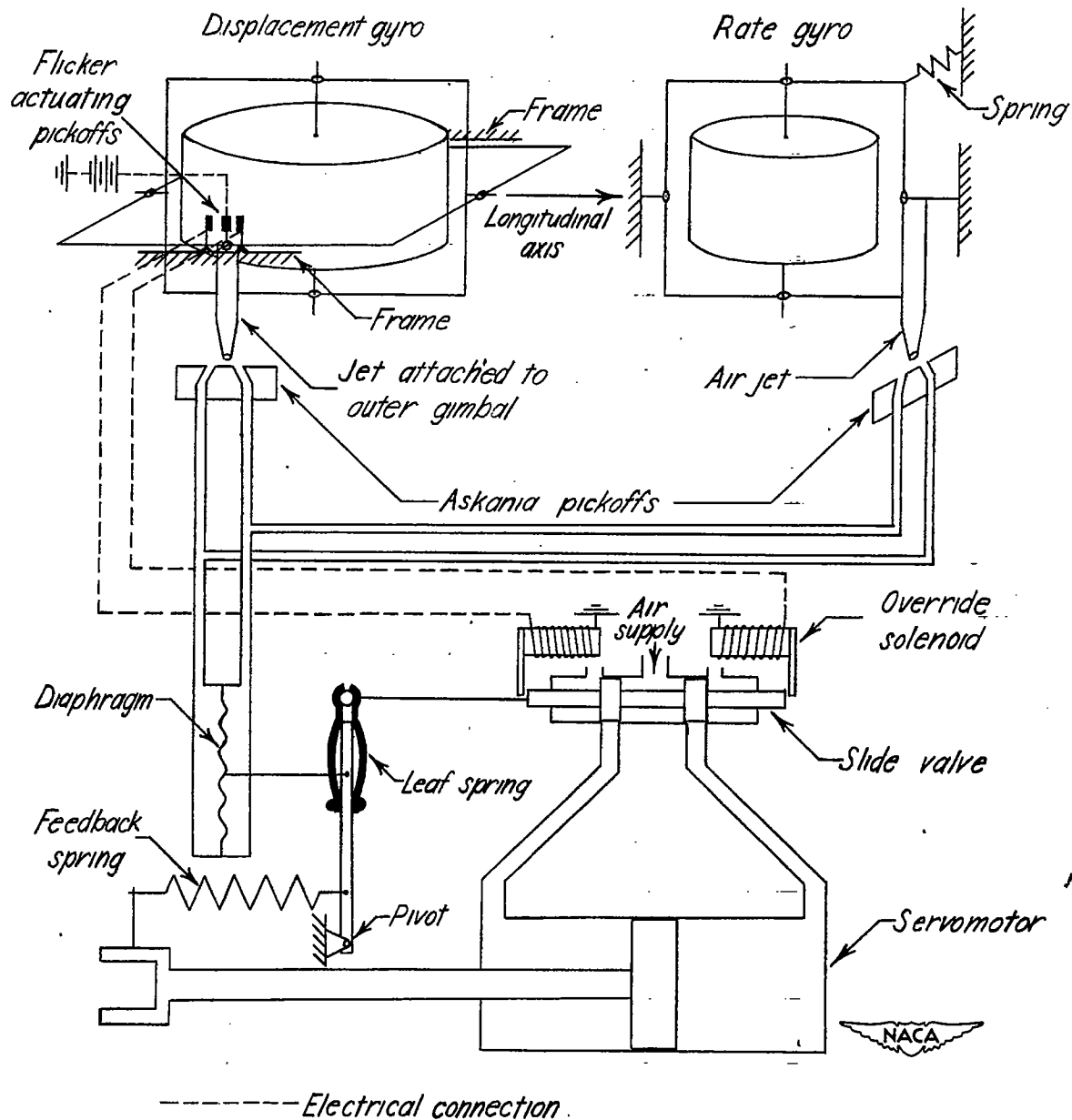
Figure 2.- Schematic diagram of a proportional-flicker autopilot system.
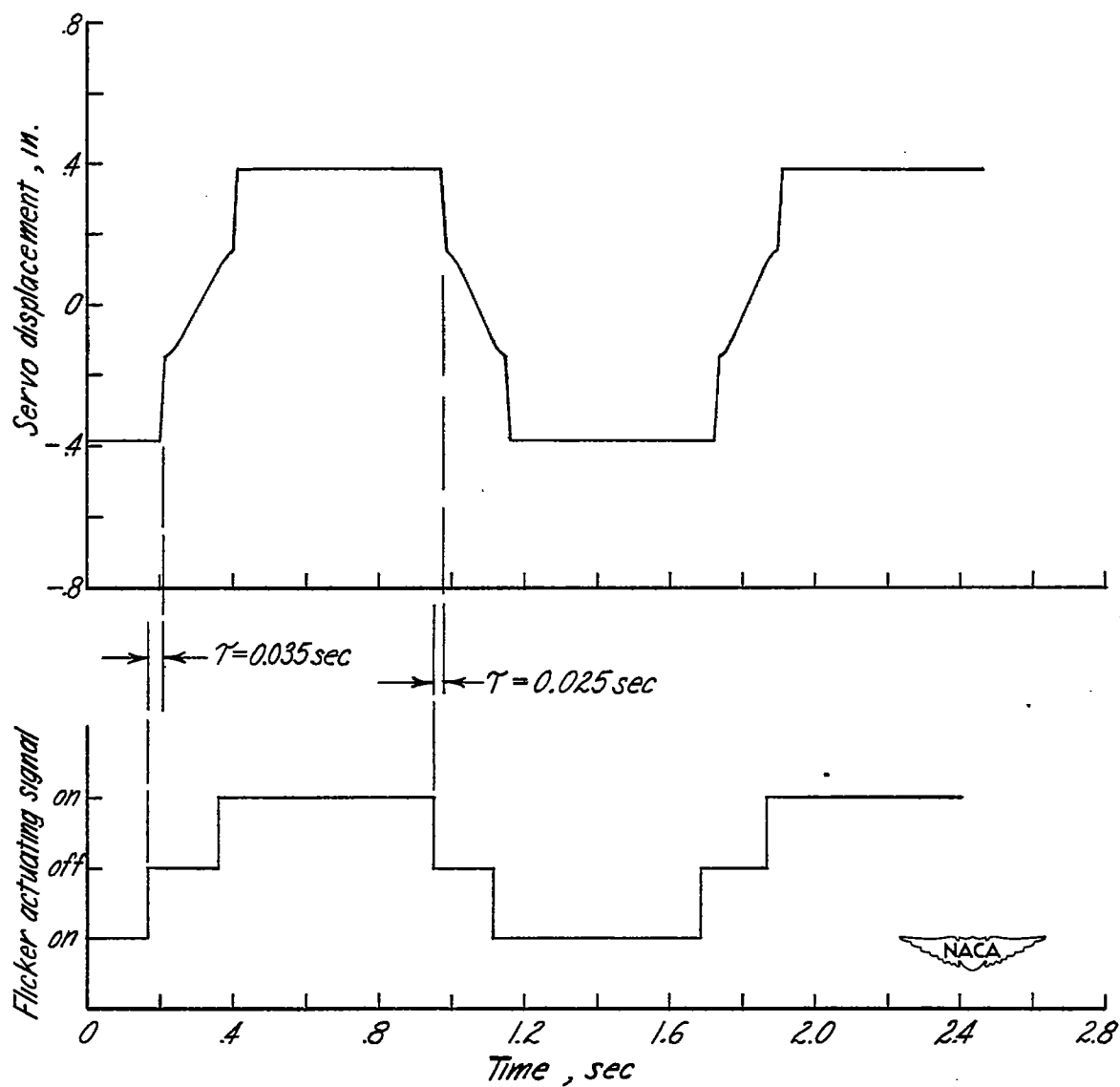
Figure 3.- Proportional-flicker servo response to a sinusoidal input signal obtained from experimental tests.
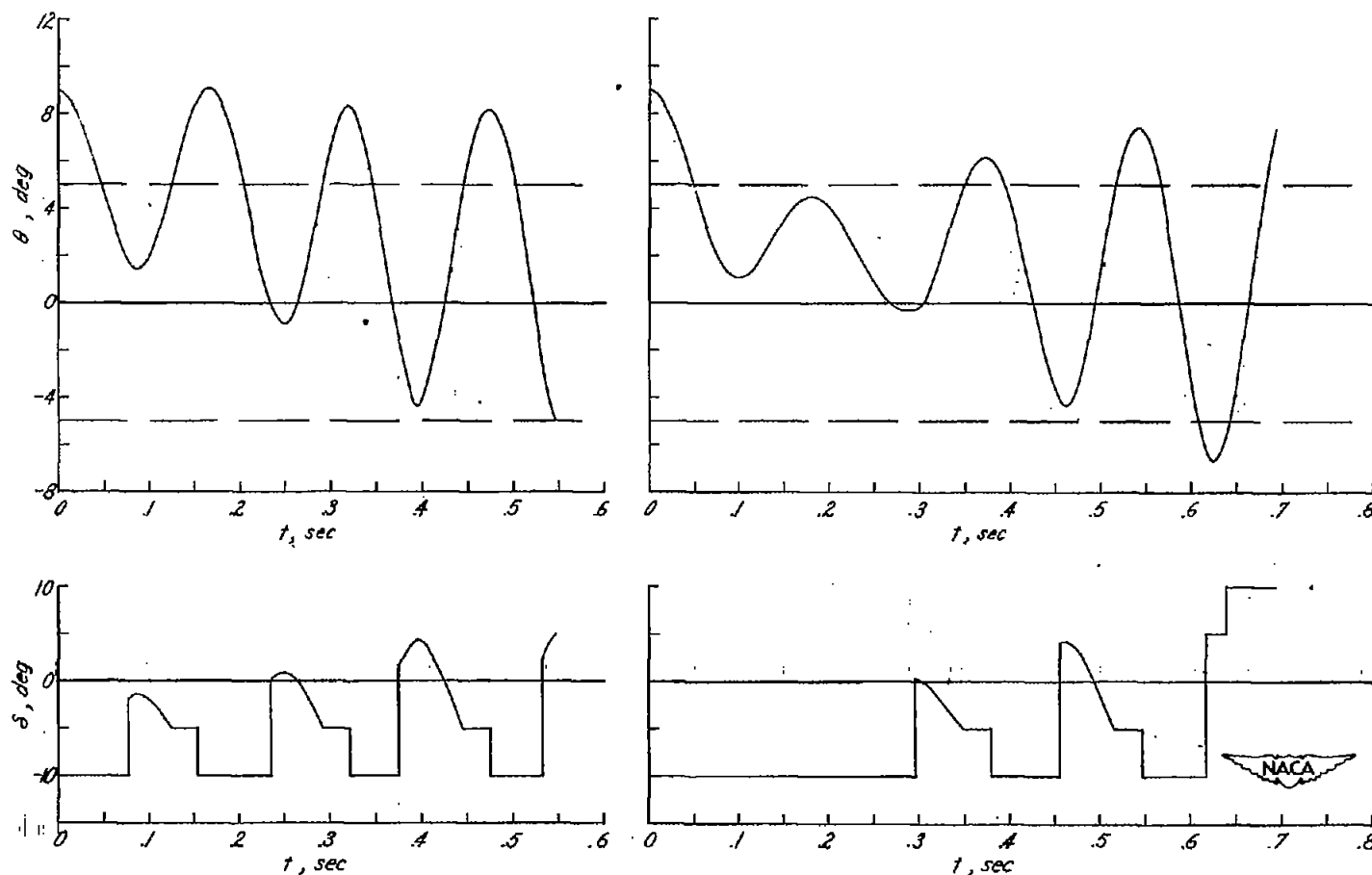
(a) End of first step at
$t_5 0 + 0.03$ second,
$K = -1$ for second step.

(b) End of first step at
$t_0 0 + 0.03$ second,
$K = -1$ for second step.

Figure 4.- Pitch transient responses to a 9° initial θ disturbance based
on sea-level flight at $M = 1.8$ and $SM = 0.86c$. Proportional band = $\pm 5^O$,
$\tau = 0.03$ second, flicker $\delta = \pm 10^O$.
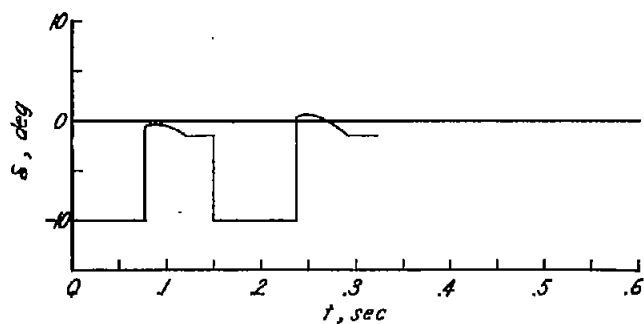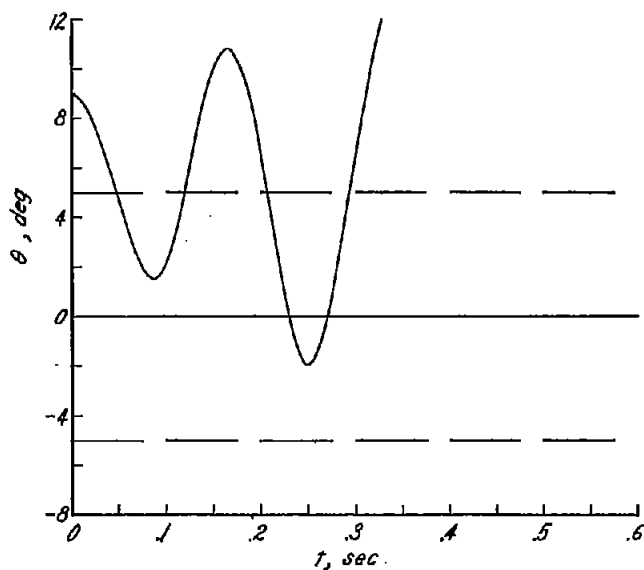
(c) End of first step at
t_{50} + 0.03 second,
K = -0.3 for second step.
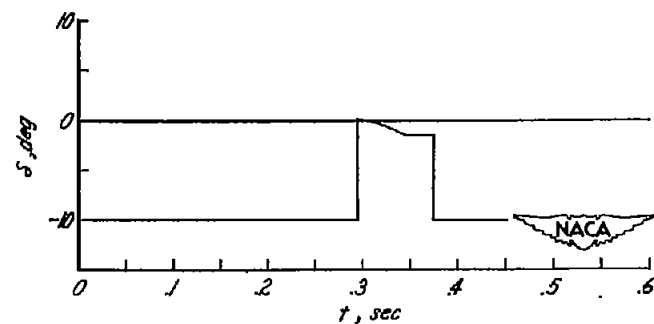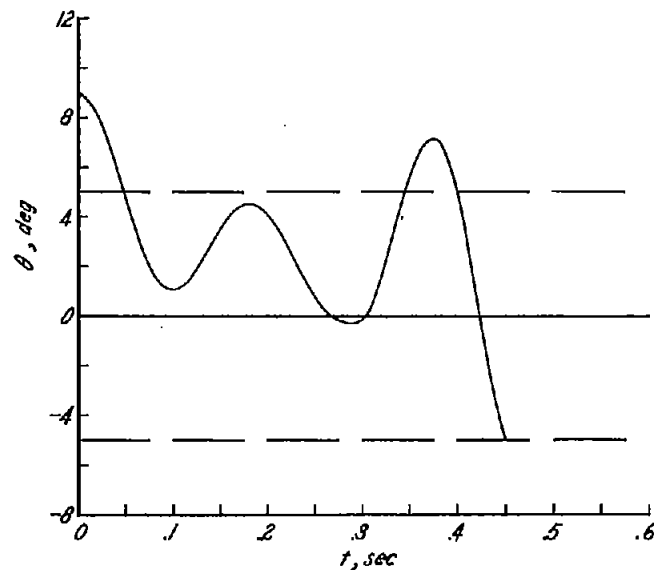
(d) End of first step at
$t_0{}^o$ + 0.03 second,
K = -0.3 for second step.

Figure 4.- Concluded.
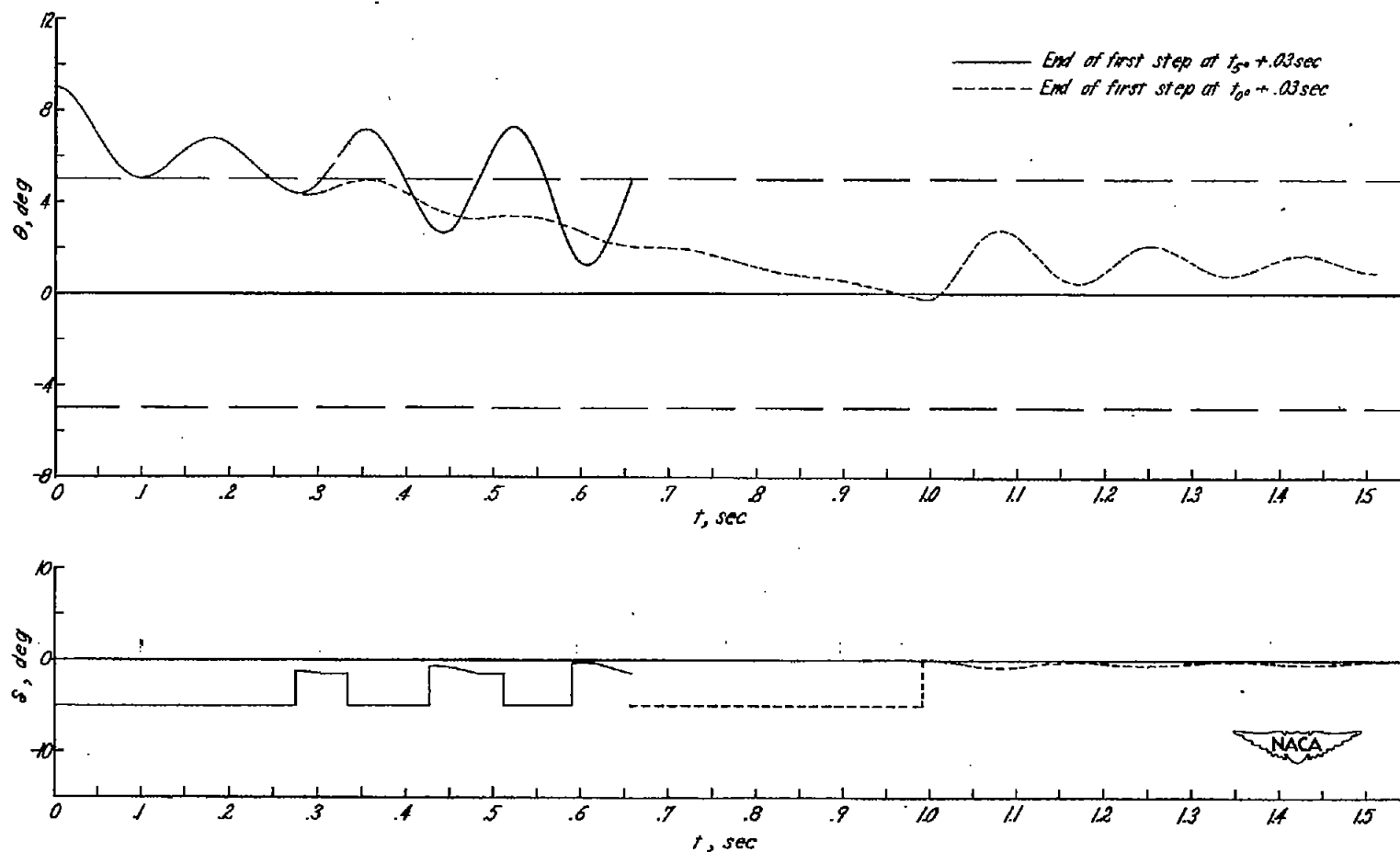
(a) Initial θ disturbance = 9°, τ = 0.03 second, proportional band = $\pm 5^{\circ}$,
K = -0.3 for second step.

Figure 5.- Pitch transient responses to an initial θ disturbance based
on sea-level flight at M = 1.8 and SM = 0.86c. Flicker δ = $\pm 5^{\circ}$.
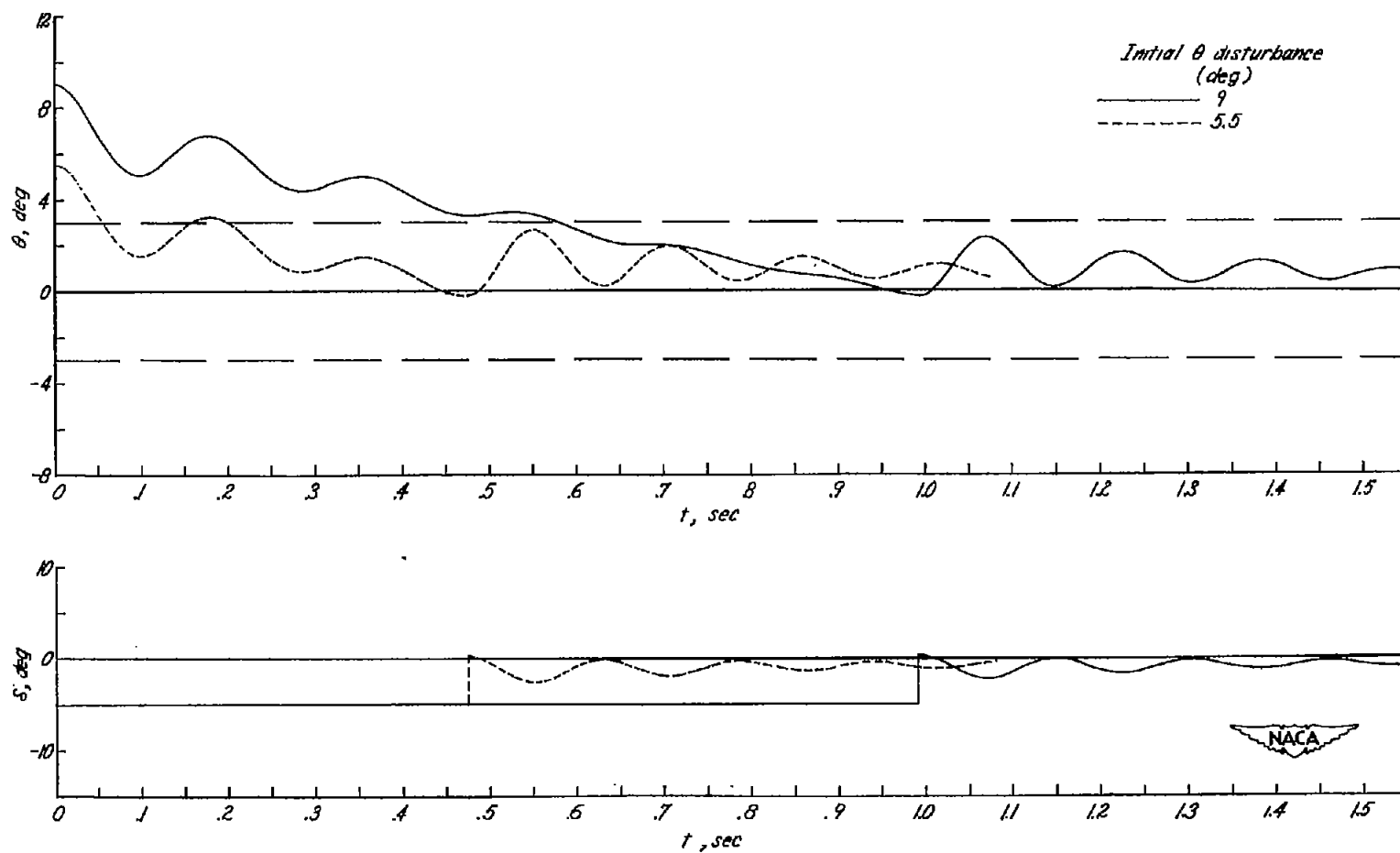
(b) τ = 0.03 second, proportional band = $\pm 3^\circ$, end of first step at t_{00} + 0.03 second, K = -1 for second step.

Figure 5.- Continued.
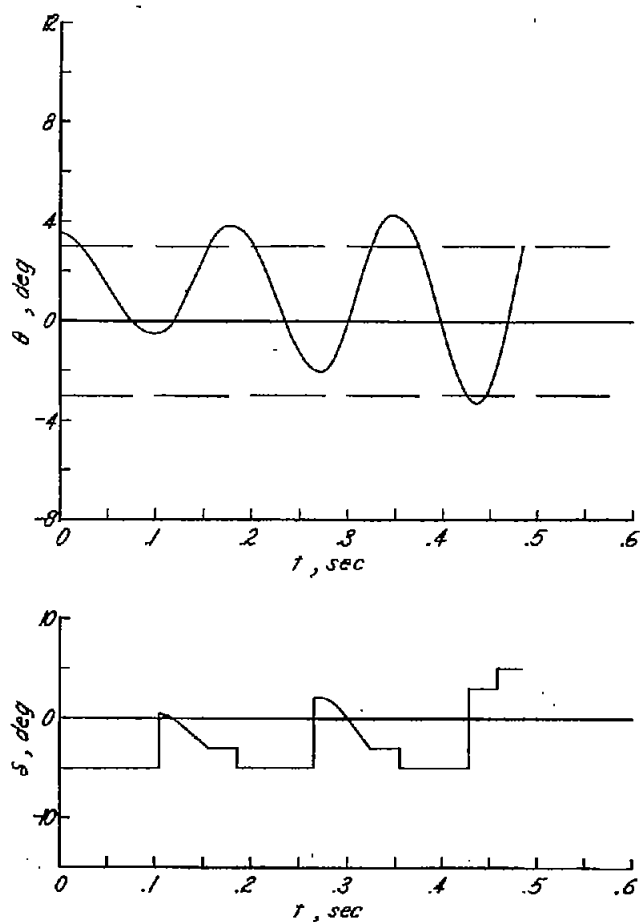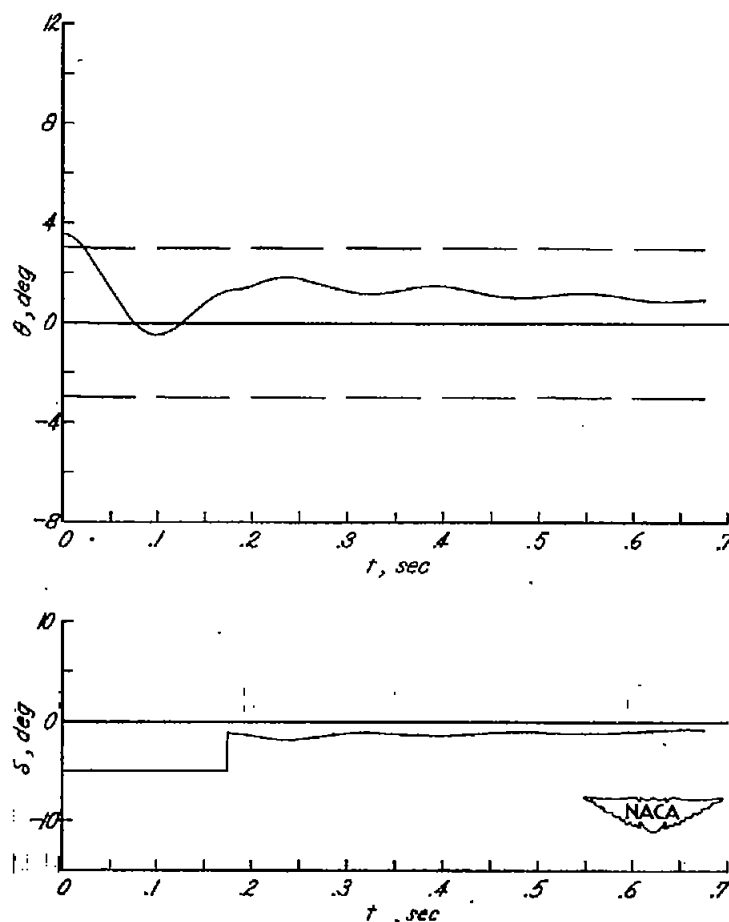
(c) Initial θ disturbance = 3.5°, τ = 0.03 second, (d) Initial θ disturbance = 3.5°, τ = 0.1 second, proportional band = ±3°, end of first step at proportional band = ±3°, end of first step at t_{0}o + 0.03 second, K = -1 for second step. t_{0}o + 0.1 second, K = -1 for second step.

Figure 5.- Concluded.
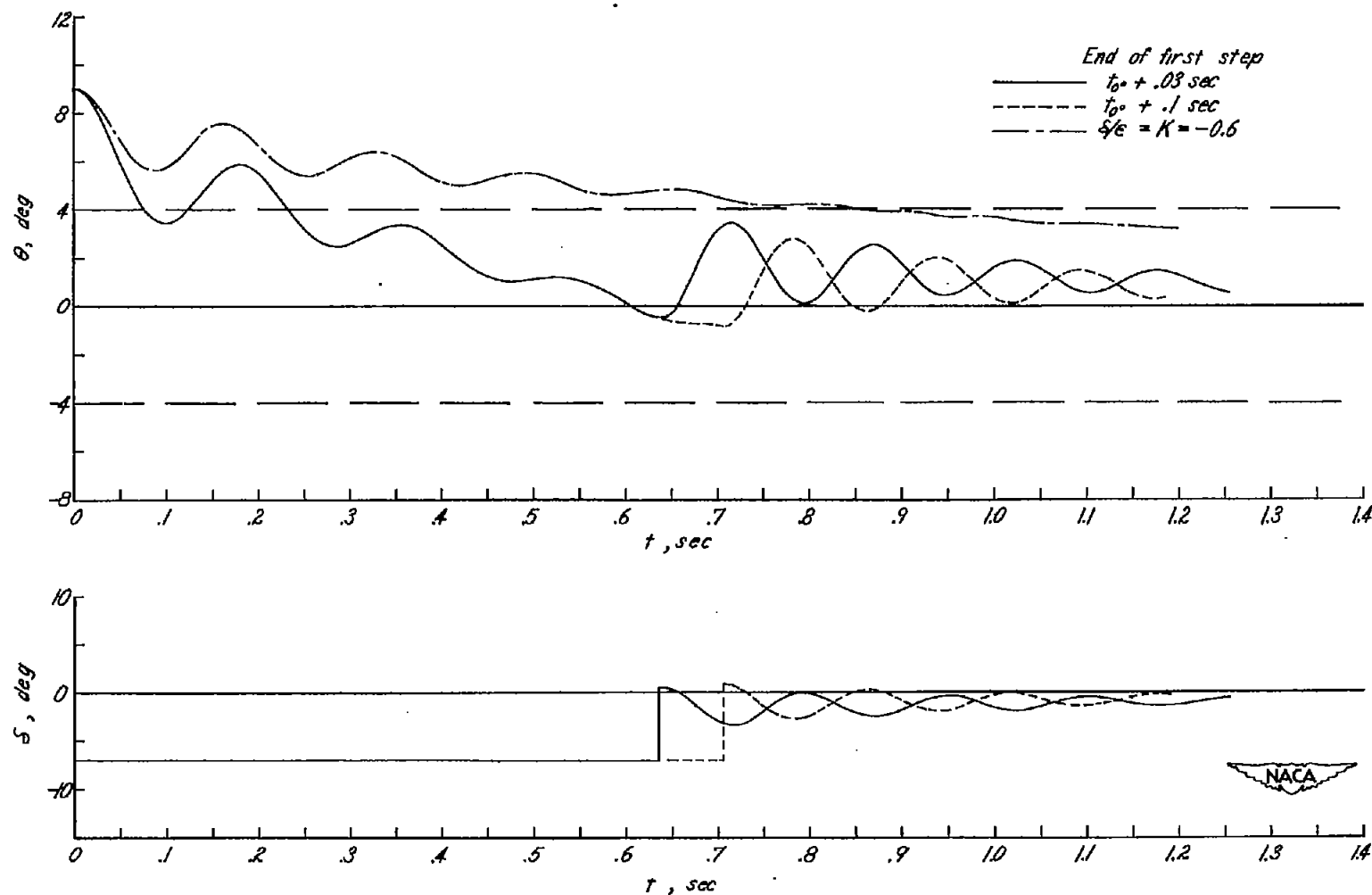
Figure 6.- Pitch transient responses to a 9° initial θ disturbance based on sea-level flight at $M = 1.8$ and $SM = 0.86c$. Proportional band = $\pm 4^\circ$, flicker $\delta = \pm 7^\circ$, $K = -1$ for second step. The calculated response of a zero-phase-lag proportional autopilot is shown for comparison.
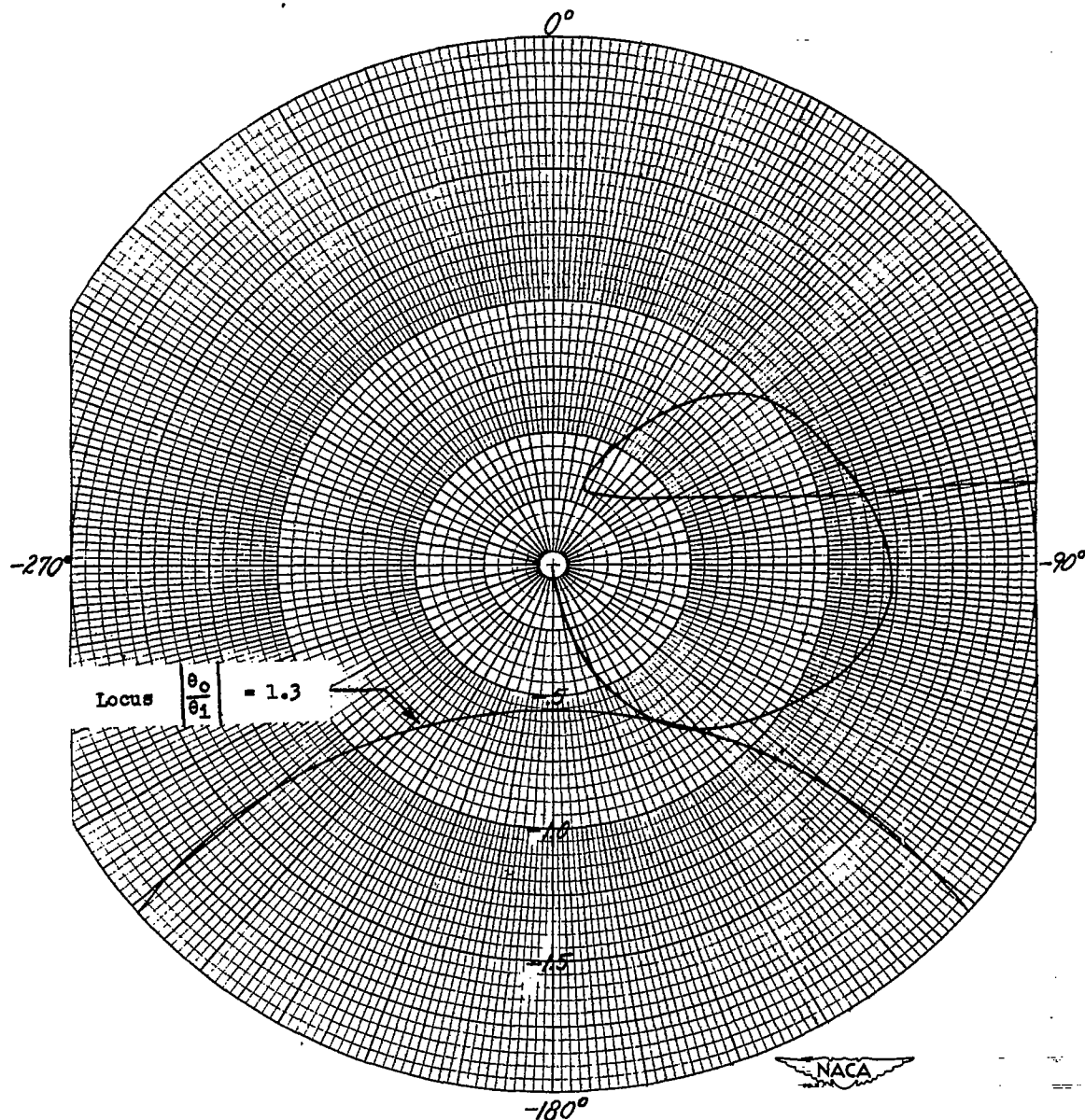
Figure 7.- Nyquist diagram for a zero-phase-lag proportional-autopilot model combination with K = -0.69 based on sea-level flight of the model and the estimated derivatives for M = 1.8 with SM = 0.86c.
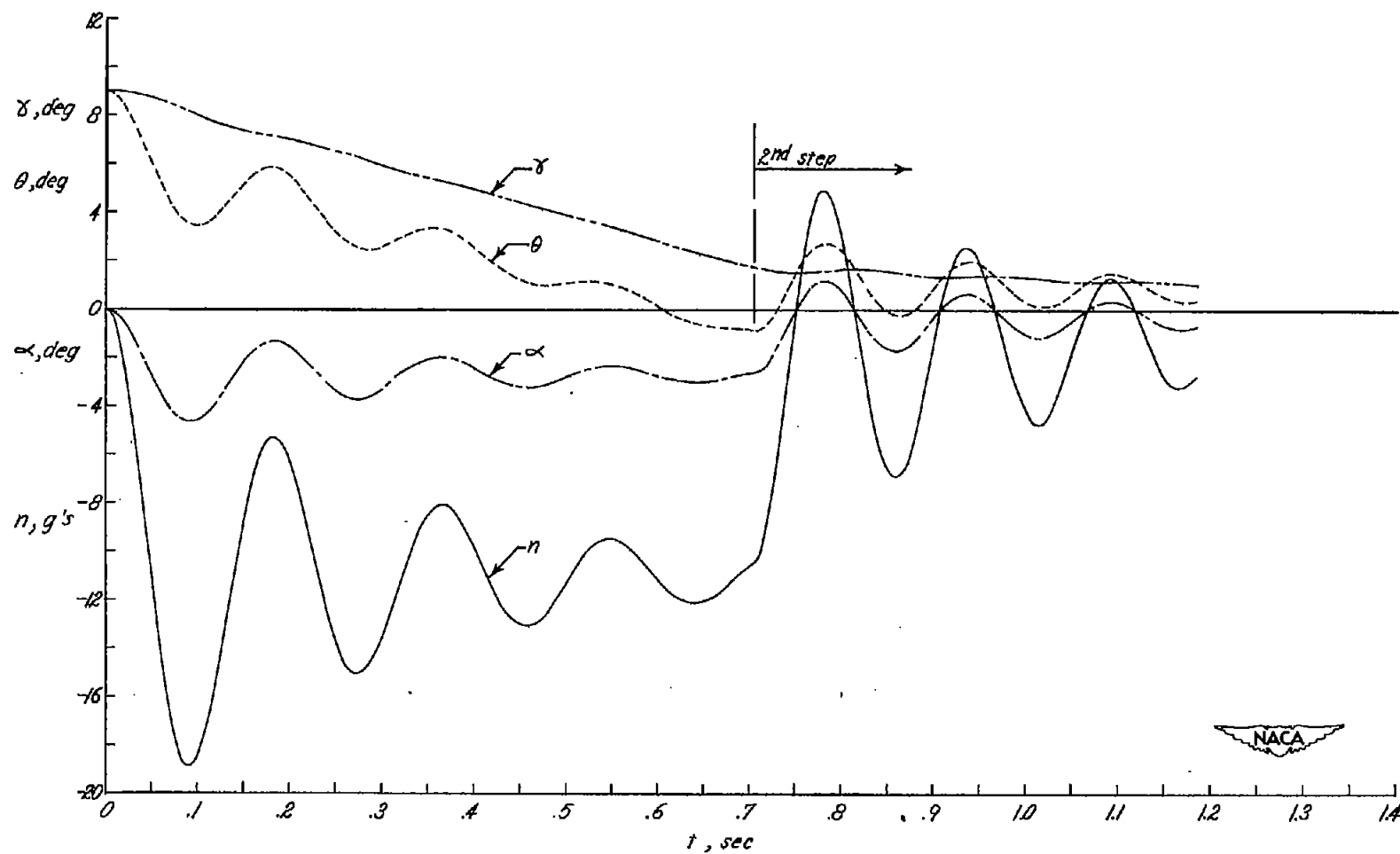
Figure 8.- Normal acceleration n and longitudinal θ, α, and γ transient responses to a 9° initial θ disturbance based on sea-level flight at M = 1.8 and SM = 0.86c. Proportional band = ±4°, flicker δ = ±7°, end of first step at t_{00} + 0.1 second, K = -1 for second step.
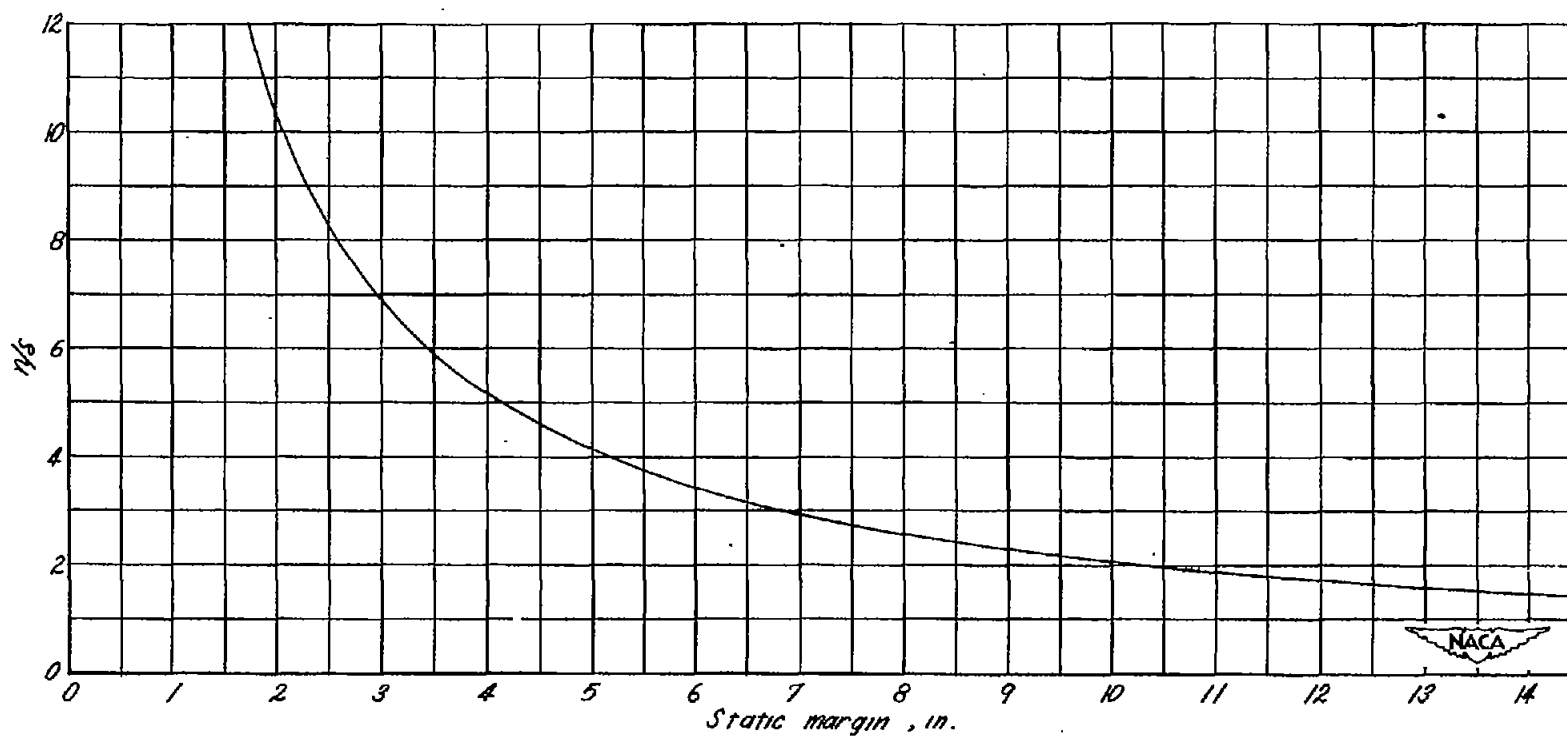
Figure 9.- The steady-state sea-level variation of n/δ with static margin
at M = 1.8 for a step δ input based on the variation of the deriva-
tives with center-of-gravity location.
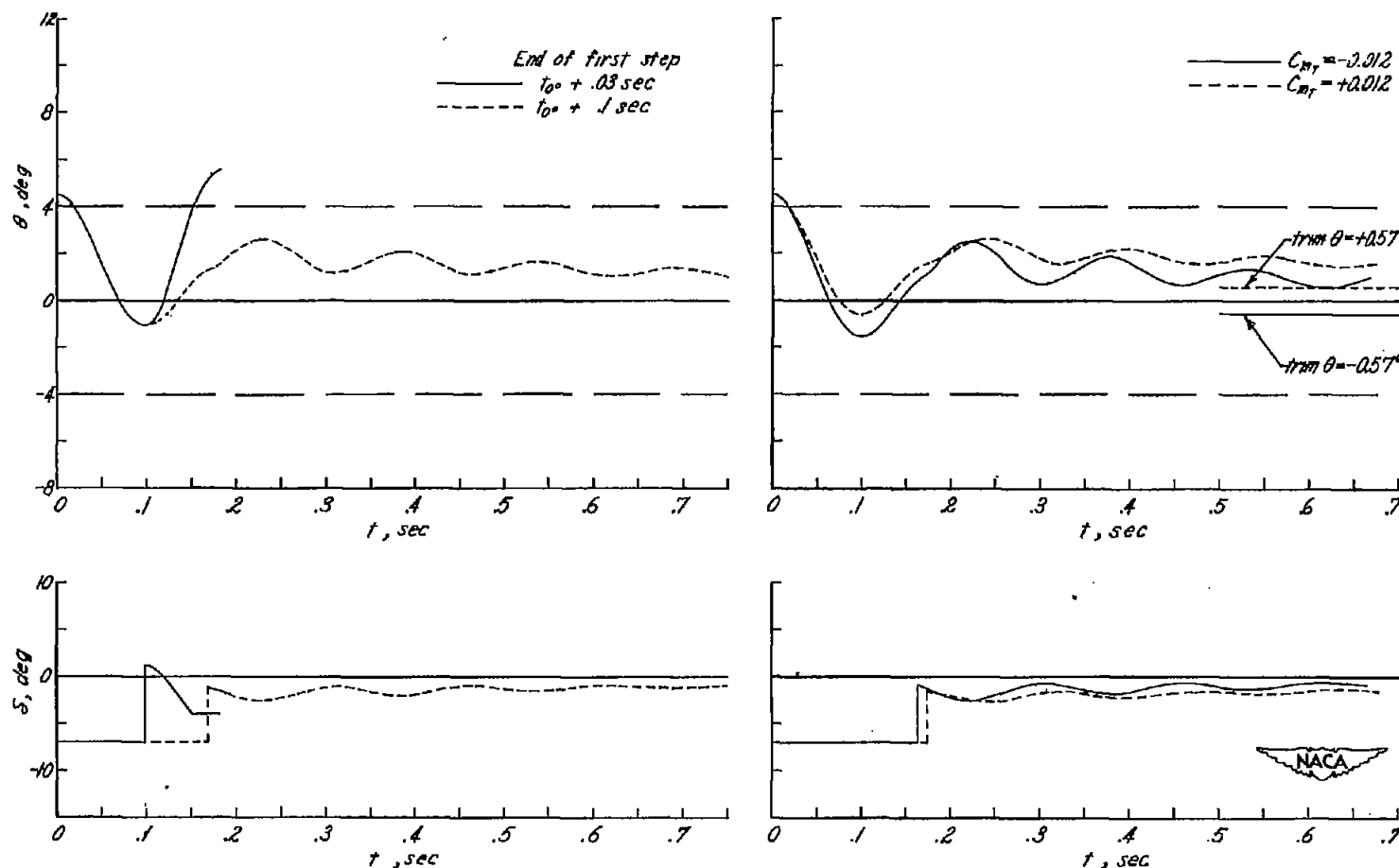
(a) No out of trim.   (b) End of first step at t_{00} + 0.1 second.

Figure 10.- The effect of an out-of-trim moment on the pitch transient responses to a 4.5° initial θ disturbance based on sea-level flight at M = 1.8 and SM = 0.86c. Proportional band = $\pm 4^\circ$, flicker $\delta = \pm 7^\circ$, K = -1 for second step.
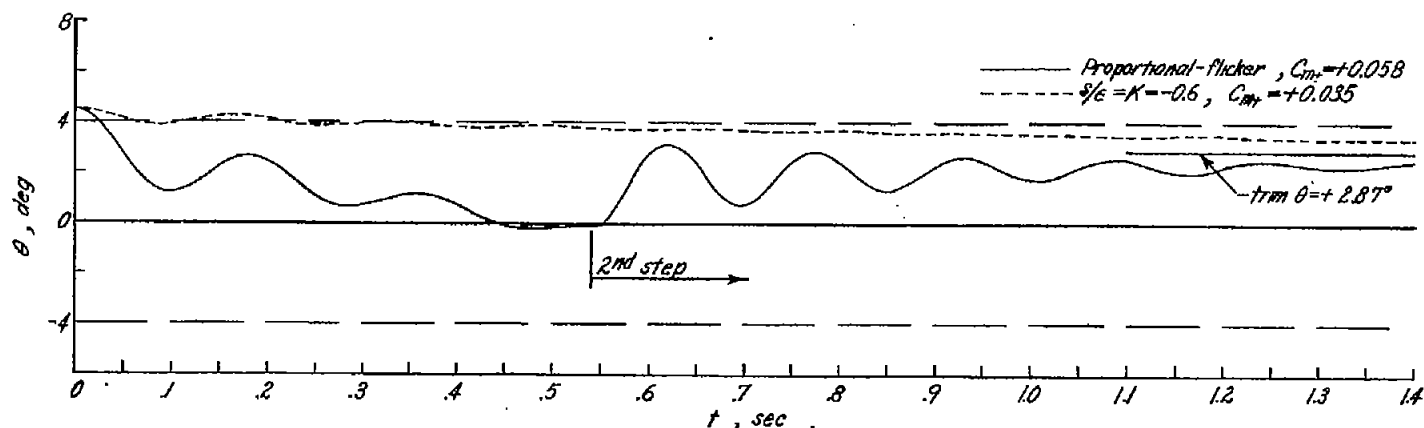
(a) Comparison of proportional-flicker autopilot with a zero-phase-lag proportional autopilot $\left(\dfrac{\delta}{\epsilon} = K\right)$ for a positive out-of-trim moment.
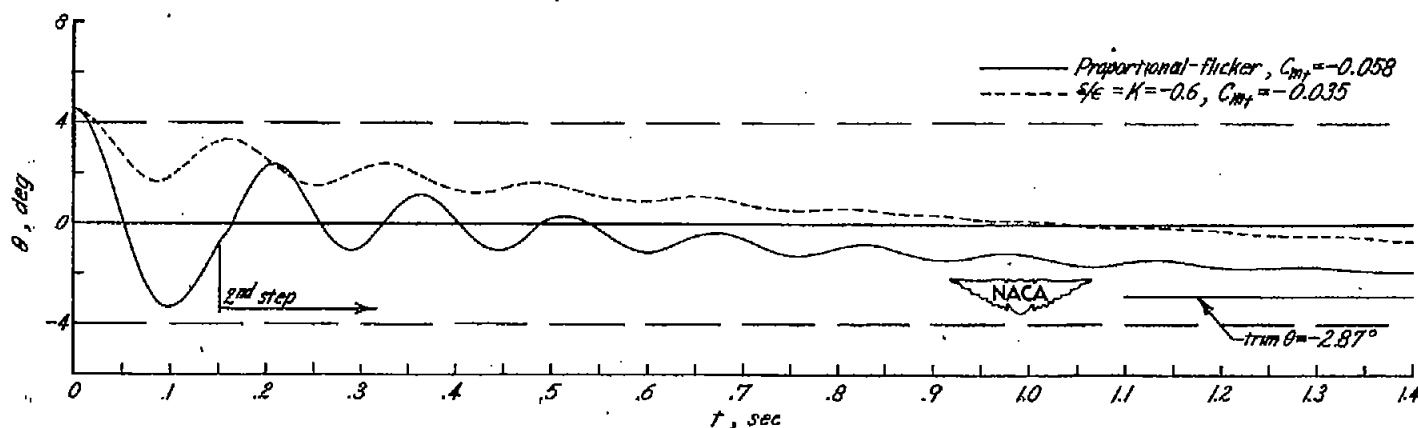
(b) Comparison of proportional-flicker autopilot with a zero-phase-lag proportional autopilot $\left(\dfrac{\delta}{\epsilon} = K\right)$ for a negative out-of-trim moment.

Figure 11.- The effect of an out-of-trim moment on the pitch transient responses to a 4.5° initial θ disturbance based on sea-level flight at $M = 1.8$ and $SM = 0.86c$. Proportional band $= \pm 4^\circ$, flicker $\delta = \pm 7^\circ$, first step ends at $t_{00} + 0.1$ second, $K = -1$ for second step.
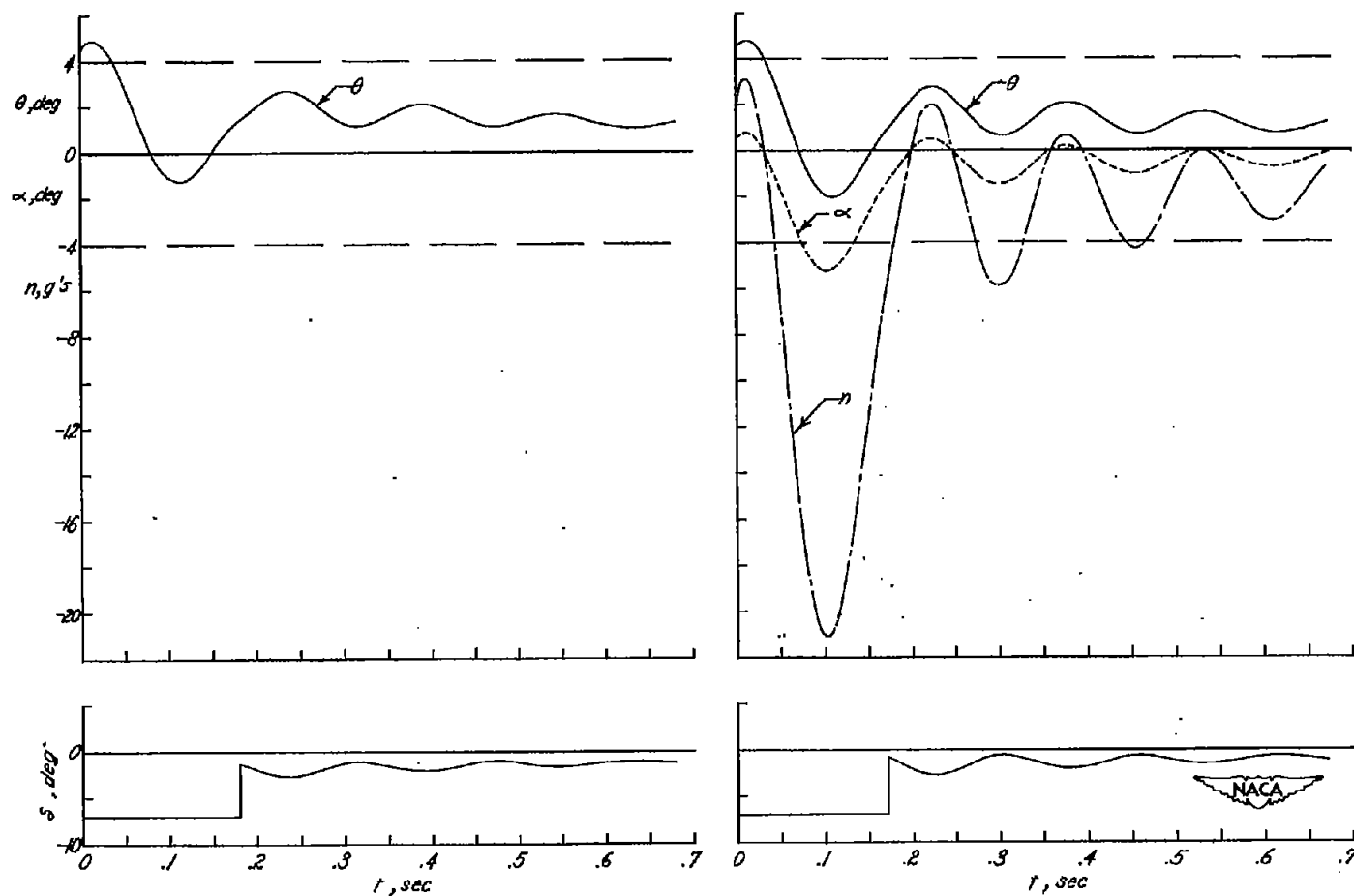
(a) $\dot{\theta}_{(0)}$ = 50 deg/sec, $\alpha_{(0)}$ = 0.   (b) $\dot{\theta}_{(0)}$ = 50 deg/sec, $\dot{\alpha}_{(0)}$ = 0.5°.

Figure 12.- Longitudinal transient responses to a 4.5° initial θ disturbance
including initial values of $\dot{\theta}$ and α ·based on sea-level flight at
M = 1.8 and SM = 0.86c. Proportional band = ±4°, flicker δ = ±7°,
first step ends at t_{Q0} + 0.1 second, K = -1 for second step.
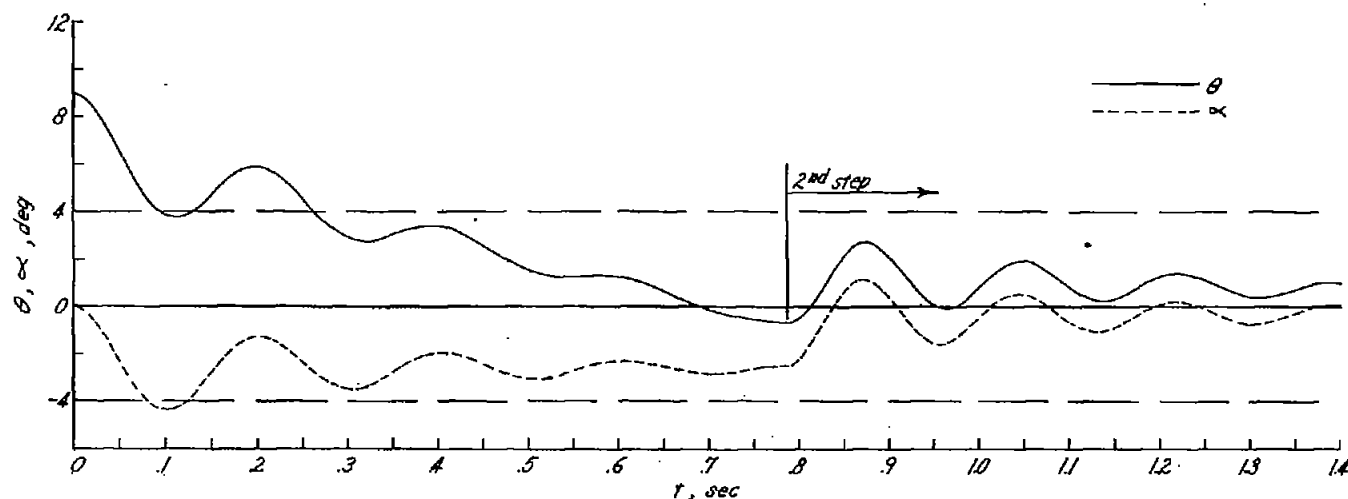
(a) Initial θ disturbance = 9°.
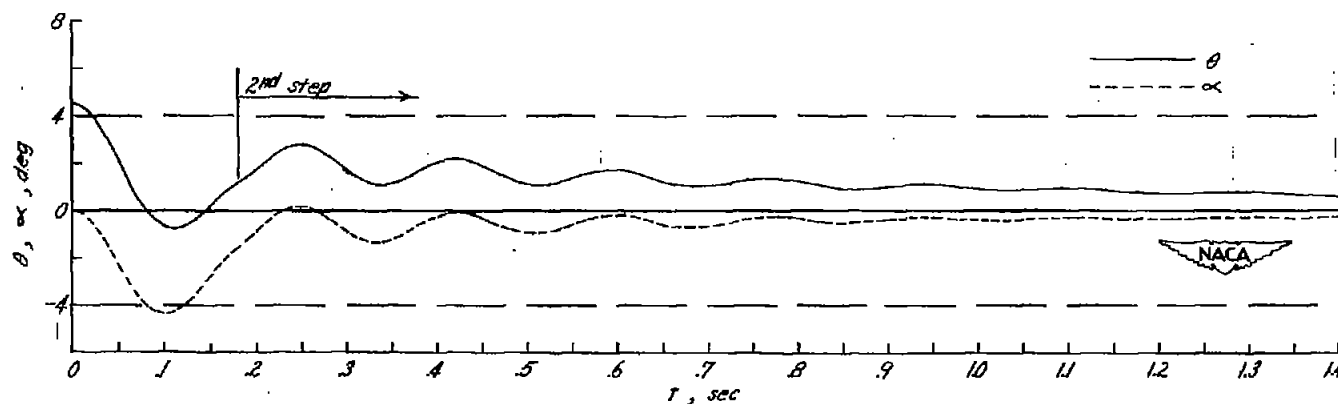
(b) Initial θ disturbance = 4.5°.

Figure 13.- Longitudinal transient responses to initial θ disturbances of 9° and 4.5° based on sea-level flight at $M = 1.4$ and $SM = 0.9c$. Proportional band = $\pm 4^{\circ}$, flicker $\delta = \pm 7^{\circ}$, end of first step at $t_{00} + 0.1$ second, $K = -1$ for second step.
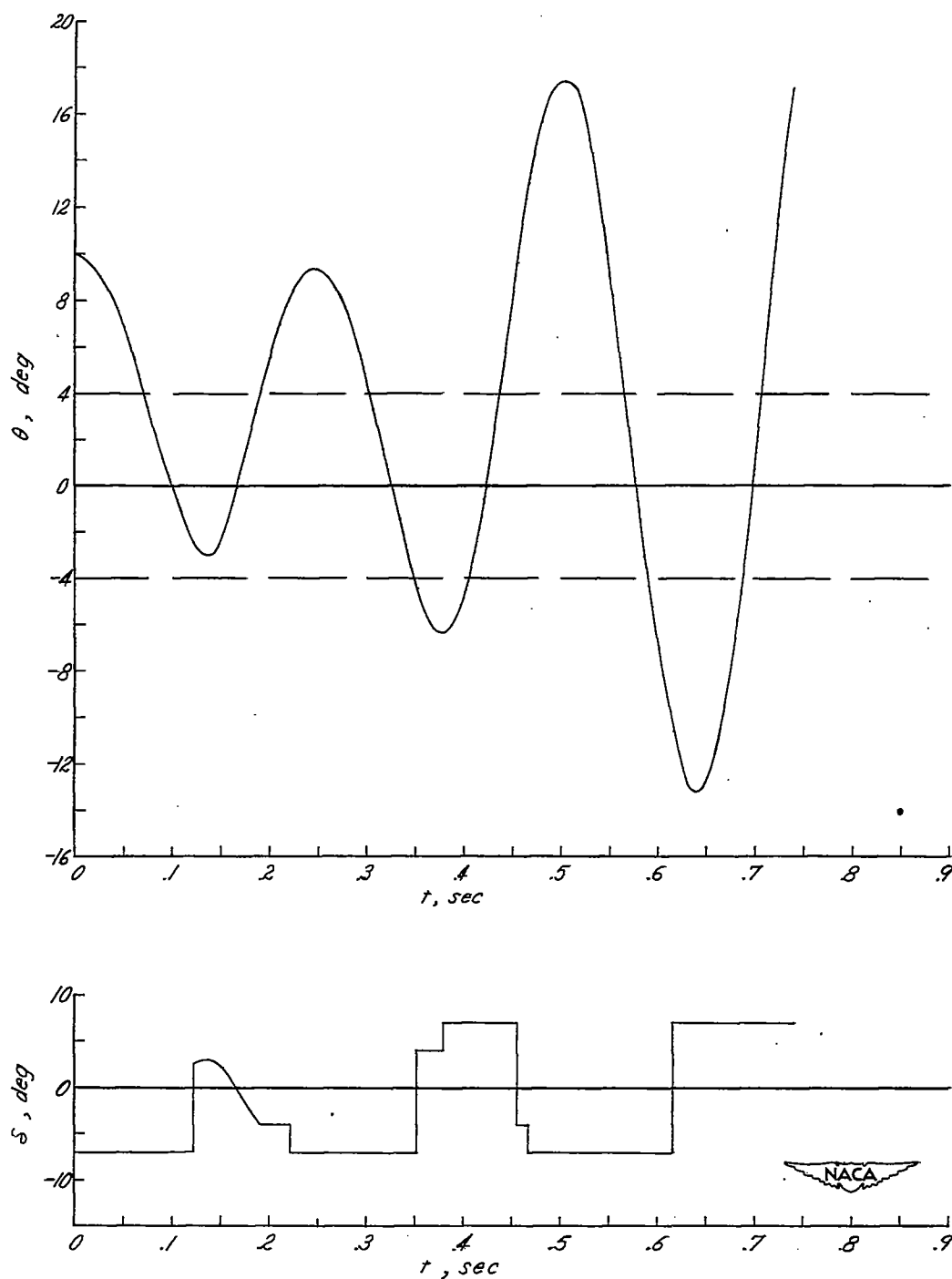
Figure 14.- Pitch transient response to a 10° initial θ disturb-
ance based on sea-level flight at $M = 1.8$ and $SM = 0.3c$.
Proportional band $= \pm 4^{\circ}$, flicker $\delta = \pm 7^{\circ}$, end of first step
at $t_{40} + 0.05$ second, $K = -1$ for second step.
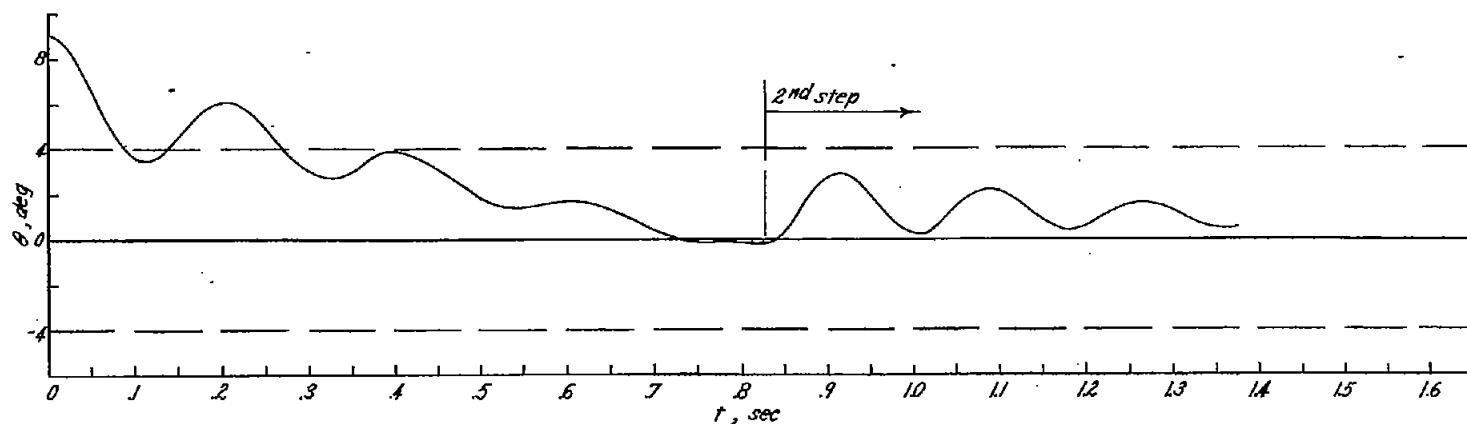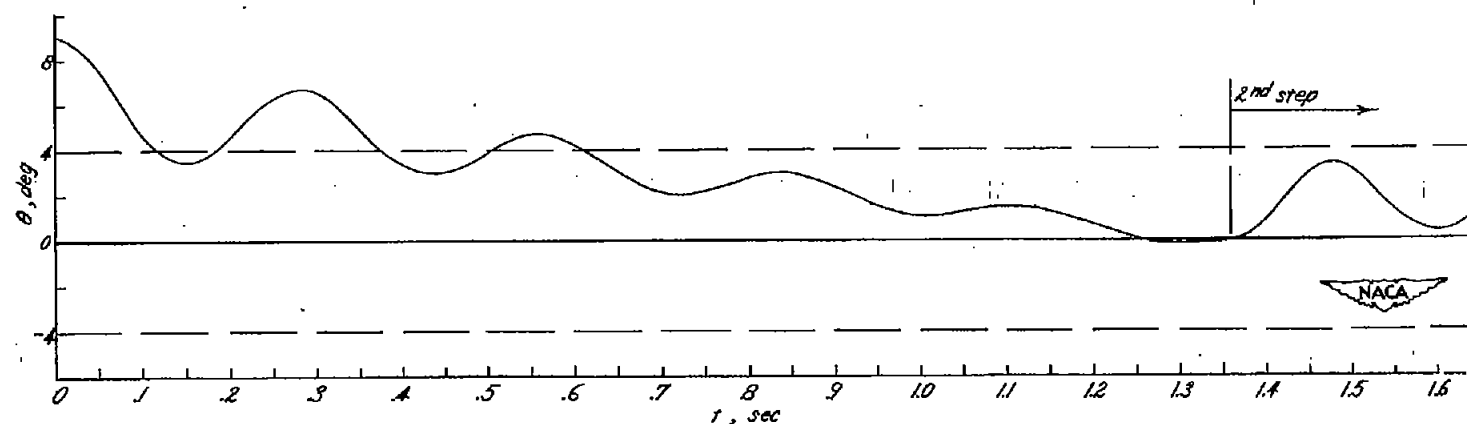
(a) 10,000 feet.

(b) 25,000 feet

Figure 15.- Pitch transient responses to 9° initial θ disturbances based on flight at 10,000 and 25,000 feet at $M = 1.8$ and $SM = 0.86c$. Proportional band $= \pm 4^\circ$, flicker $\delta = \pm 7^\circ$, end of first step at $t_{00} + 0.1$ second, $K = -1$ for second step.
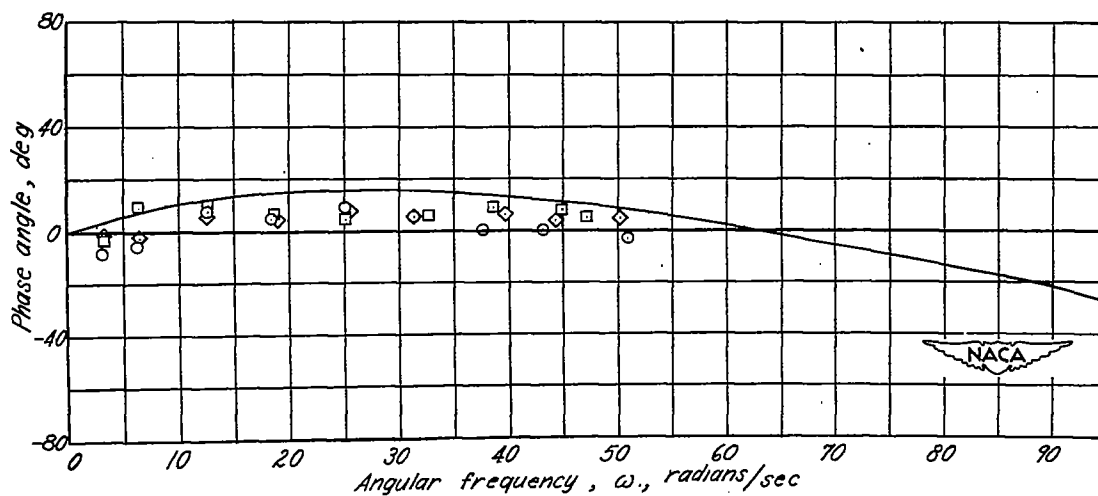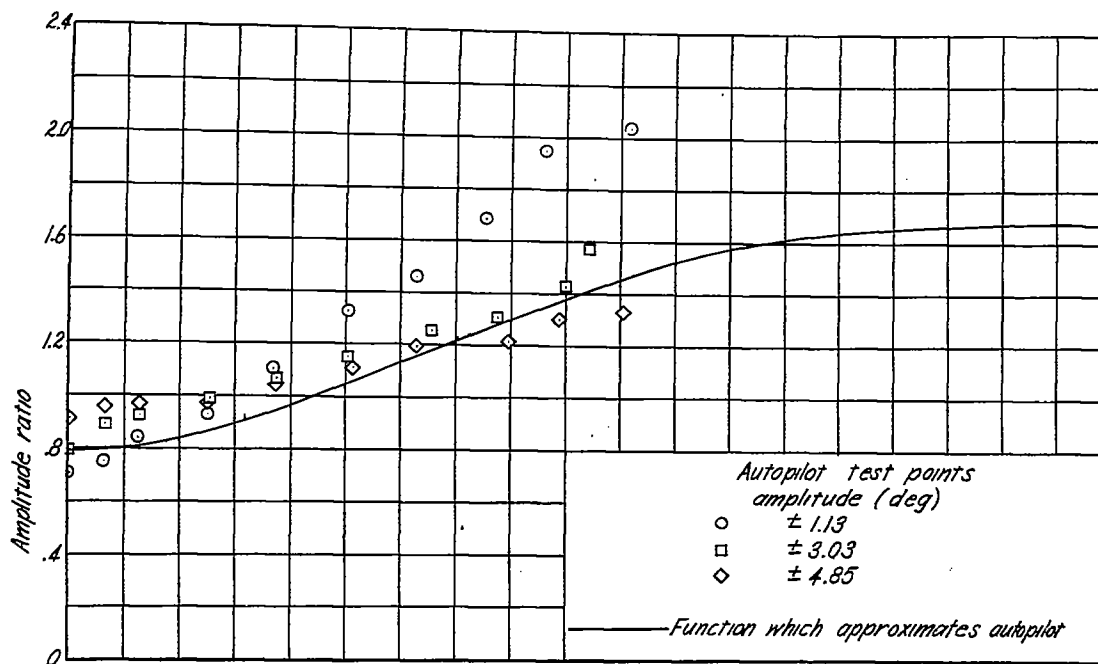
(a) Amplitude and phase response of the approximate autopilot function
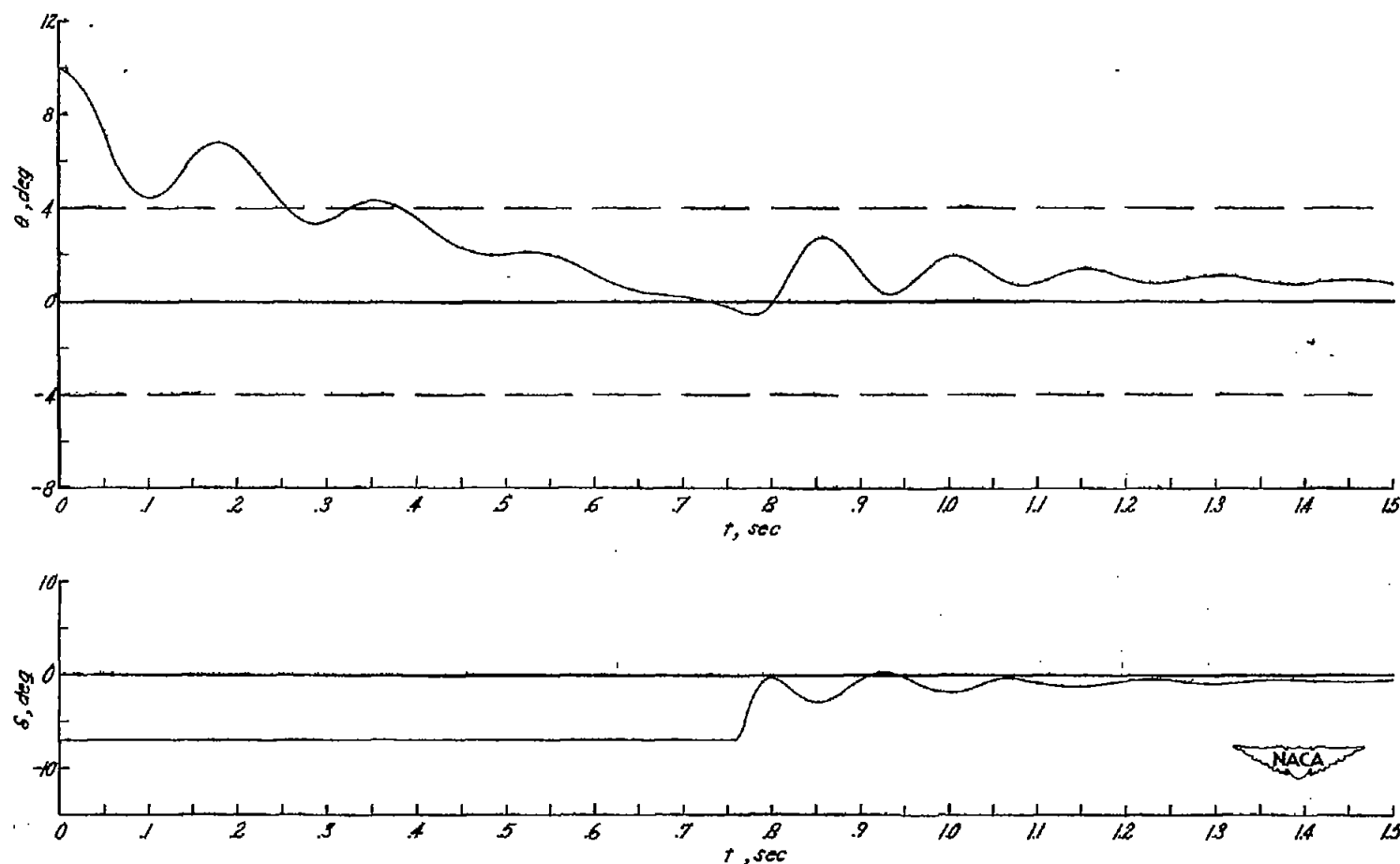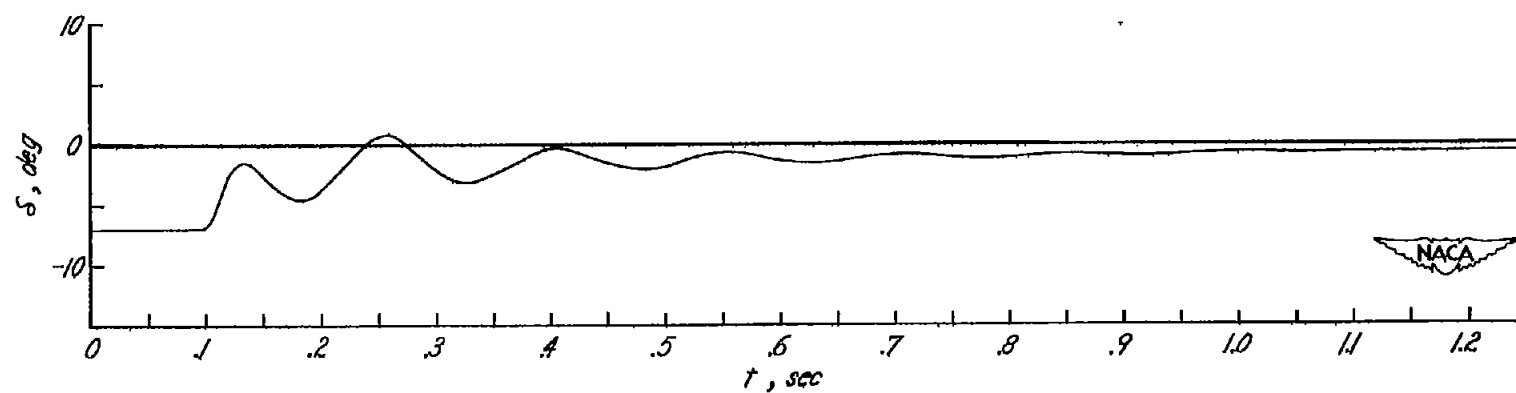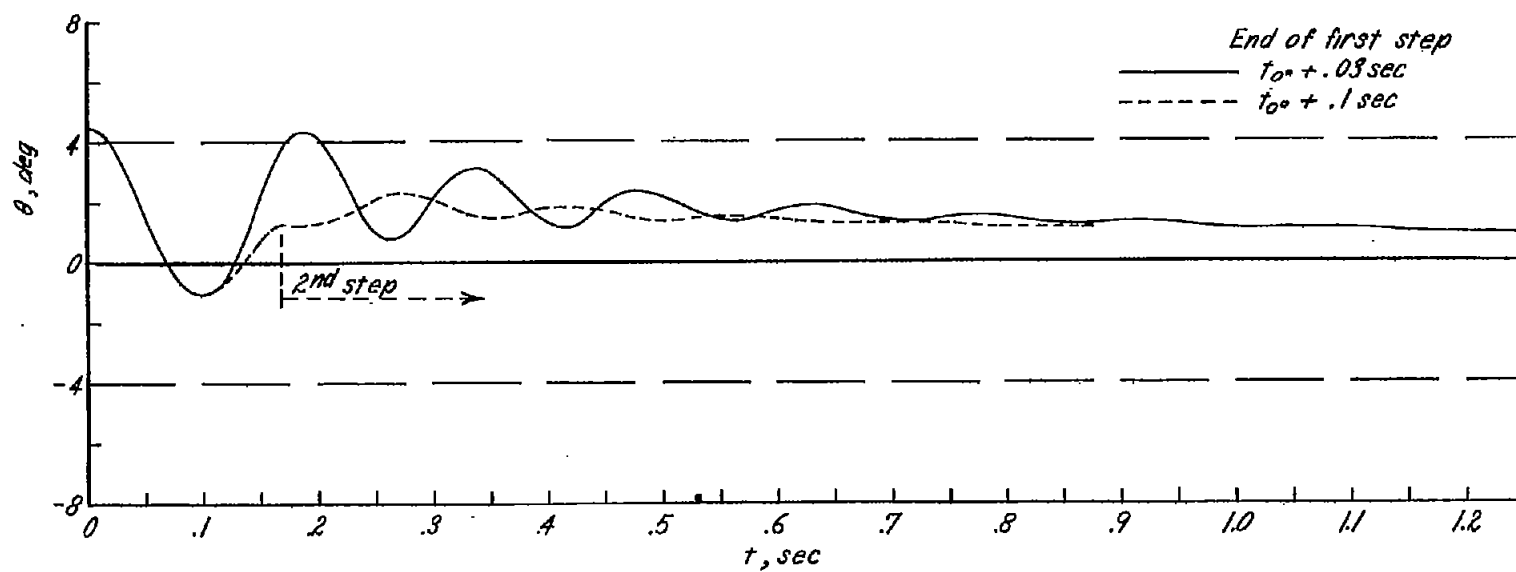and of the actual autopilot test points.

Figure 16.- Comparison of the function which approximates the proportional
part of the proportional-flicker autopilot with the autopilot test
points based on the amplitude and phase response of a proportional-
flicker servo obtained from oscillating-table tests of a V-1 displace-
ment and rate gyroscope.
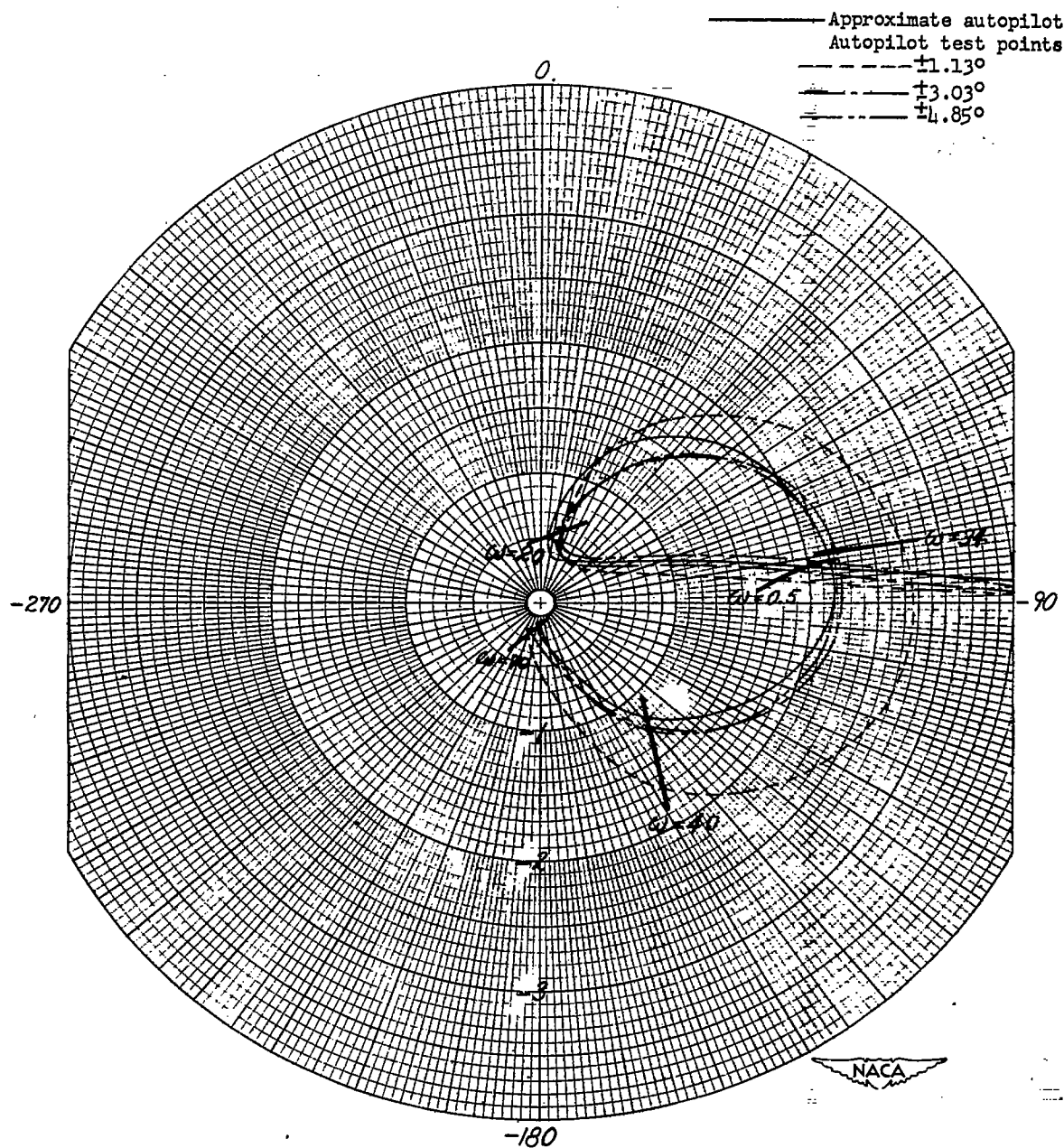
(b) Nyquist diagrams for approximate autopilot function-model combination and for longitudinal pitch oscillation amplitudes of $\pm1.13°$, $\pm3.03°$, and $\pm4.85°$ based on sea-level flight at $M = 1.8$ and $SM = 0.86c$.

Figure 16.- Concluded.
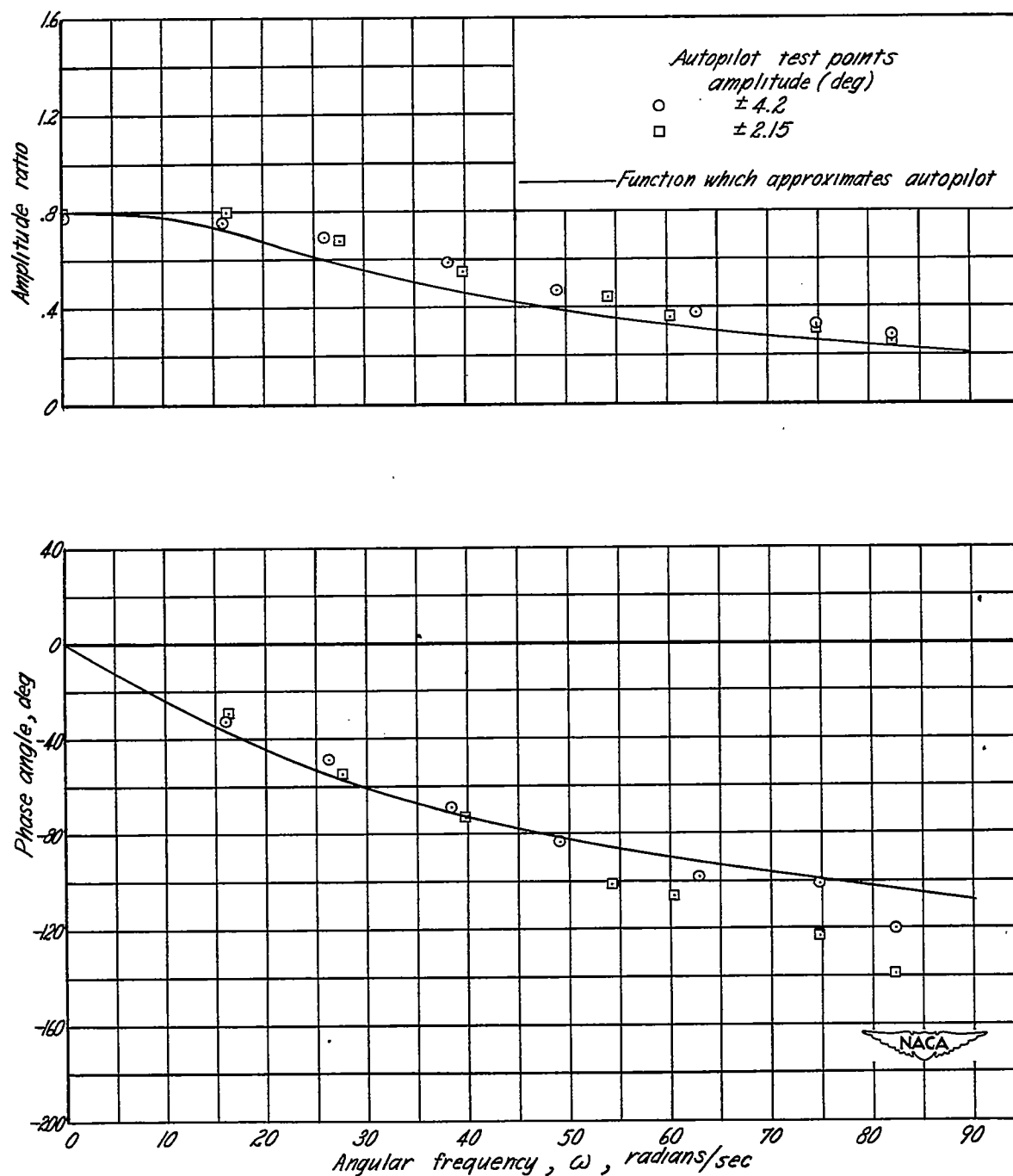
Figure 17.- Comparison of the function which approximates the proportional
part of the proportional-flicker autopilot with the autopilot test
points based on the amplitude and phase response of the servo obtained
from oscillating-table tests of a displacement gyroscope only.

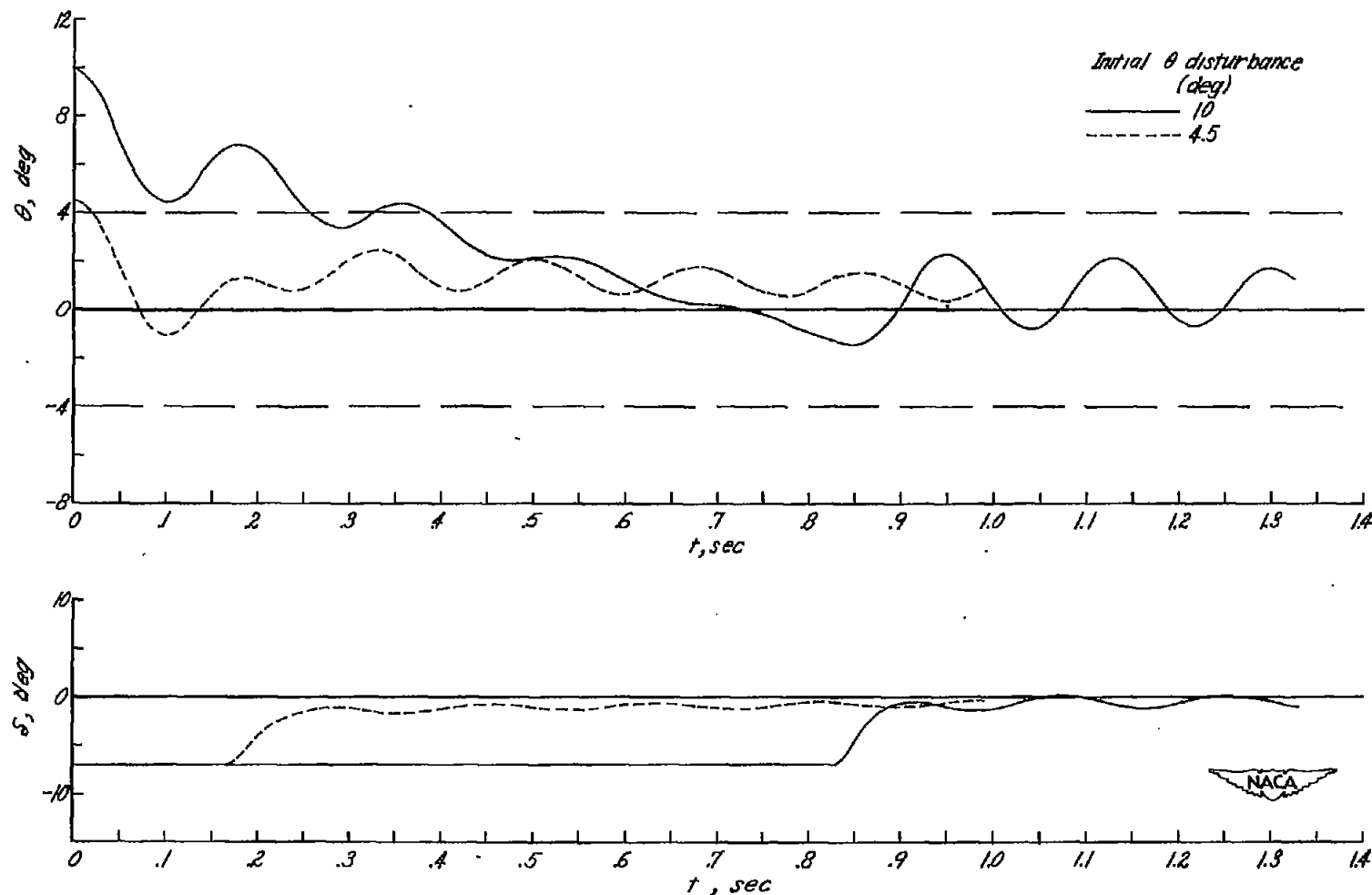(a) Initial θ disturbance = 10°, end of first step at $t_{0}o$ + 0.03 second.

Figure 18.- Pitch transient responses to an initial θ disturbance based on sea-level flight at M = 1.8 and SM = 0.86c. Proportional band = $\pm 4^o$, flicker δ = $\pm 7^o$, $\frac{\delta}{\epsilon}$ = f(D) for second step including displacement-plus-rate signal.

(b) Initial θ disturbance = 4.5°.

Figure 18.- Continued.
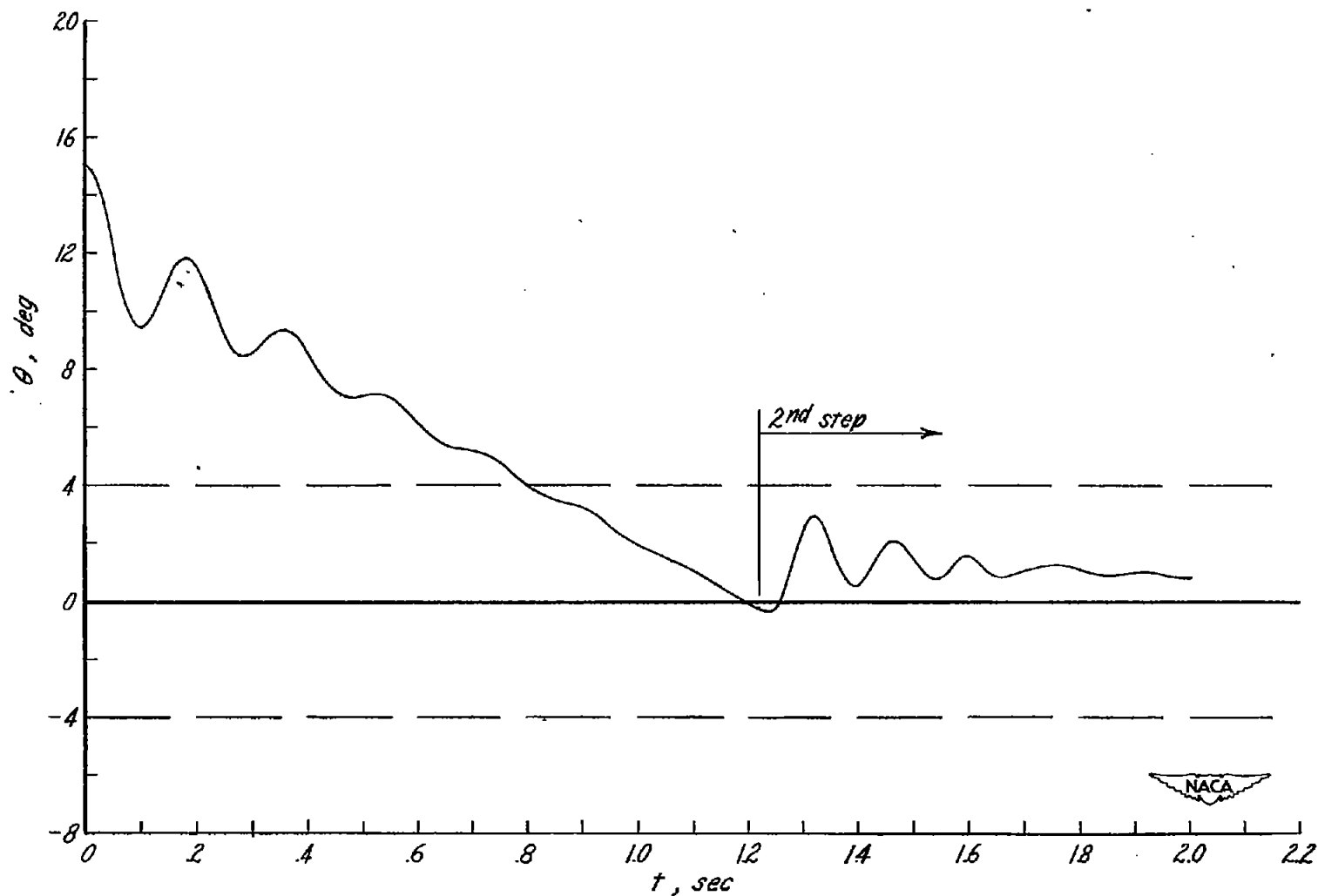
(c) Initial θ disturbance = 15°, end of first step at $t_{0}0 + 0.03$ second.
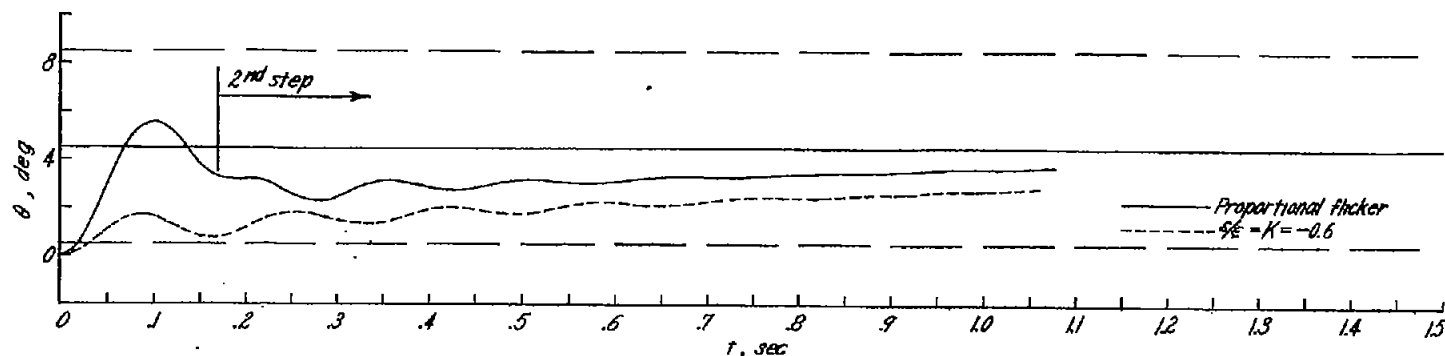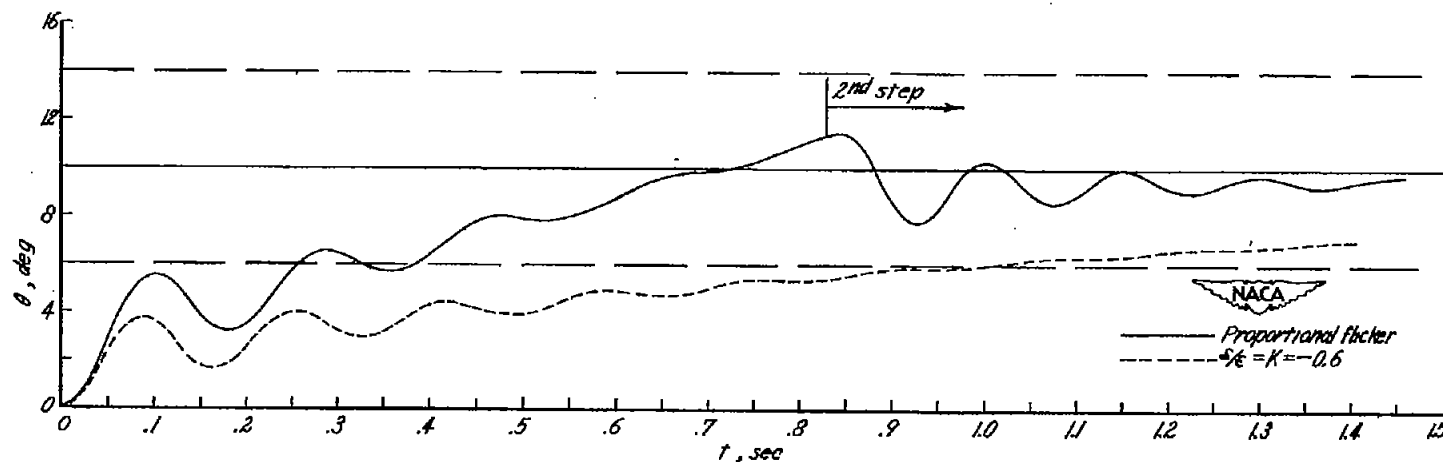
Figure 18.- Concluded.

Figure 19.- Pitch transient responses to 10° and 4.5^{o} initial θ disturbances based on sea-level flight at $M = 1.8$ with $SM = 0.86c$. Proportional band $= \pm 4^{o}$, flicker $\delta = \pm 7^{o}$, end of first step at $t_{0}^{o} + 0.1$ second, $\frac{\delta}{\epsilon} = f(D)$ for second step using displacement signal only.

(a) New neutral point = 4.5°, end of first step at $t_{4.5°}$ + 0.1 second.

(b) New neutral point = 10°, end of first step at $t_{10°}$ + 0.1 second.

Figure 20.- Pitch transient responses to 4.5° and 10° command signals based on sea-level flight at $M = 1.8$ with $SM = 0.86c$. Proportional band = ±4°, flicker $\delta = ±7°$, $\frac{\delta}{\epsilon} = f(D)$ for second

step including displacement-plus-rate signal. The responses of a zero-phase-lag proportional autopilot are shown for comparison.